DEVELOPMENT OF CONCRETE-BASED SOLAR CHIMNEY CONFIGURATIONS INTEGRATED WITH THERMOELECTRIC MODULES

MR. TAMNARN TAPRAKONE

A DISSERTATION SUBMITTED IN PARTIAL FULFILLMENT OF THE REQUIREMENTS
FOR THE DEGREE OF DOCTOR OF PHILOSOPHY IN
ENERGY ENGINEERING TECHNOLOGY
DEPARTMENT OF POWER ENGINEERING TECHNOLOGY
GRADUATE COLLEGE
KING MONGKUT'S UNIVERSITY OF TECHNOLOGY NORTH BANGKOK
ACADEMIC YEAR 2026
COPYRIGHT OF KING MONGKUT'S UNIVERSITY OF TECHNOLOGY NORTH BANGKOK

DEVELOPMENT OF CONCRETE-BASED SOLAR CHIMNEY CONFIGURATIONS INTEGRATED WITH THERMOELECTRIC MODULES

MR. TAMNARN TAPRAKONE

A DISSERTATION SUBMITTED IN PARTIAL FULFILLMENT OF THE REQUIREMENTS
FOR THE DEGREE OF DOCTOR OF PHILOSOPHY IN
ENERGY ENGINEERING TECHNOLOGY
DEPARTMENT OF POWER ENGINEERING TECHNOLOGY
GRADUATE COLLEGE
KING MONGKUT'S UNIVERSITY OF TECHNOLOGY NORTH BANGKOK
ACADEMIC YEAR 2026
COPYRIGHT OF KING MONGKUT'S UNIVERSITY OF TECHNOLOGY NORTH BANGKOK



Dissertation Certificate

The Graduate College, King Mongkut's University of Technology North Bangkok

Title DEVELOPMENT OF CONCRETE-BASED SOLAR CHIMNEY CONFIGURATIONS INTEGRATED WITH THERMOELECTRIC MODULES

By Mr. Tamnarn Taprakone

Accepted by the Graduate College, King Mongkut's University of Technology North Bangkok in Partial Fulfillment of the Requirements for the Doctor of Philosophy in Energy Engineering Technology

..... Acting Dean, Graduate College

(Professor Dr. Saowanit Sukparungsee)

Dissertation Examination Committee

..... Chairman

(Professor Dr. Joseph Khedari)

..... Advisor

(Associate Professor Dr. Preeda Chantawong)

..... Committee

(Associate Professor Dr. Chatchan Thongjub)

..... Committee

(Assistant Professor Dr. Dusit Ngamrungroj)

..... Committee

(Assistant Professor Acting Sub Lt. Dr. Chaiyot Damrongkijkosol)

Name : Mr. Tamnarn Taprakone
Dissertation Title : DEVELOPMENT OF CONCRETE-BASED SOLAR CHIMNEY CONFIGURATIONS INTEGRATED WITH THERMOELECTRIC MODULES
Major Field : Energy Engineering Technology
King Mongkut's University of Technology North Bangkok
Dissertation Advisor : Associate Professor Dr. Preeda Chantawong
Academic Year : 2026

ABSTRACT

The growing challenges of thermal discomfort, elevated indoor heat gain, and increasing electricity demand in tropical residential buildings have heightened interest in passive cooling and building-integrated energy technologies.

This thesis presents extensive field investigation of concrete-based solar chimney configurations integratedwith thermoelectric modules to generate electrical current using the stored heat in the roof and wall built using local commercial materials widely used for residential houses.More precisely, the aim is to experimentally examines the thermal and ventilation performance of roof and wall concrete-based solar chimney integrated with thermoelectric power generation and compare them to a conventional fiber-cement roof and wall configurations in the hot-humid climate of Thailand.

Different solar chimeny configurations are considered. The first is a Concrete Roof Solar Chimney made from undulating fiber-cement panels with Thermoelectric modules (CSRCT). Several cases were investigations by varying the number (one and ten) and alignment of TE modules. Also, two options were adopted for cooling the thermoelectric modules either naturally by the chimney induced ventilation or assisted using two small DC fans connected directly to a small Photovoltaic (PV) panel. The second series considered a Lightweight Solar Wall Chimney with a thermoelectric module (LSWCT).The thermal performances of these different configurations of concrete-based solar chimneys are compared to a Simple fiber-cement Roof (SFR) and a Simple Cement Wall (SCW) configuration respectively.

Field tests were conducted using two small houses (2.016 m^3; 1.2 m x1.2 m x 1.2 m) built using white-painted fiber cement and gypsum boards for the walls. The concrete roof faced south. The CSRCT design included two small openings at the inlet and outlet to allow ventilation. To act as a thermoelectric generator (TEG), CSRCT and LSWCTtwo series of tests were conducted by installing one and ten (model MT2-1,6-127) with dimensions of 40 mm x 40 mm on the ventilated side of the concrete roof and lightweight wall.

Solar radiation, indoor, roof and wall surface temperatures, heat flux, airflow, and thermoelectric output over a typical daytime operating period were conituously recorded and analysed. The findings indicate that the CSRCT and LSWCT configurations substantially reduced roof heat conduction by approximately 29.3 %–78.8% compared to the SCR roof and SCW wall, while enhancing natural ventilation, with internal airflow increasing from 0.01–0.015 m/s to 0.013–0.75 m/s. Indoor air temperatures in the RSCCT and LSWCT houses were consistently 0.2–2.8°C lower than those in the reference structure, thereby confirming the effectiveness of buoyancy-driven airflow in alleviating attic heat accumulation.

Thermoelectric modules generated between 0.12 and 1.8 mWand 0.04 to 3.16 mW power generated by the TEGs of supplementary electrical power, demonstrating the viability of simultaneous passive cooling and small-scale energy harvesting from roof surface heat. These findings underscore the RSCCT and LSWCT as practical, low-complexity, and energy-conserving roof and wall modification strategies for enhancing thermal comfort, reducing cooling loads, and promoting solar-assisted natural ventilation in tropical buildings. Future developments will focus on design optimization, scalability, and long-term performance assessment for real residential applications.

Finally, this thesis demonstrated that all-concrete roof and lightweight wall configurations not only help transfer unwanted heat out of the house but also induce ventilation, which improves indoor thermal comfort and generates electrical current. The various proposed configurations of concrete roofs and lightweight walls can be applied to low-cost residential houses, offering a viable alternative for harvesting thermal energy in concrete roofs and wall buildings.

(Total 57 Pages)

Keywords : roof solar concrete chimney; lightweight solar wall chimney; save energy; heat gain reduction; thermoelectric power generation; building cooling

มหาวิทยาลัยเทคโนโลยีพระจอมเกล้าพระนครเหนือ

_____ Advisor

ACKNOWLEDGEMENTS

This research study was successfully completed due to the generous assistance of Associate Professor Dr.Preeda Chantawong, my advisor. He provided valuable advice, reviewed the content and research methods, and provided valuable feedback, particularly on the outline and guidelines for writing the content and analysis, as well as setting a timeframe for presenting progress. This provided significant motivation for me. I am deeply grateful and appreciative of his kindness, and I express my sincere gratitude to him.

I would like to express my sincere gratitude to Professor Dr.Joseph Khedari, Associate Professor Dr.Chatchan Thongchap, Assistant Professor Dr.Dusit Ngamrungroj, and Assistant Professor Acting Second Lieutenant Chaiyot Damrongkitkoson for their generous time as chairperson and the thesis defense committee. Their guidance, advice, and observations enabled me to develop my work and consider various issues more thoroughly, leading to the successful completion of this thesis.

Finally, I would like to express my gratitude to all persons who have helped explicitly or implicitly to the achievement of my dissertation, and my family members for continuous and generous support as well as all friends during my study..

Tamnarn Taprakone

TABLE OF CONTENTS

Page

ABSTRACT ..... **ii**
ACKNOWLEDGEMENTS ..... **iv**
TABLE OF CONTENTS ..... **v**
LIST OF TABLES ..... **vi**
LIST OF FIGURES ..... **vii**
CHAPTER 1 INTRODUCTION **1**
1.1 Background 1
1.2 Objective 2
1.3 Scopes of study 2
1.4 Expected outcome 3
CHAPTER 2 LITERATURE REVIEW AND THEORETICAL CONSIDERATION **4**
2.1 Climate and thermal challenges in tropical housing 4
2.2 Thermal insulation and radiant barriers in roofing 4
2.3 Passive cooling and natural ventilation techniques 5
2.4 Solar chimney designs 6
2.5 Thermoelectric modules in building applications 11
2.6 Literature Review 14
CHAPTER 3 EXPERIMENTAL SETUP AND METHODOLOGY **20**
3.1 The roof solar concrete chimney integrated with thermoelectric modules 20
3.2 The roof solar concrete chimney integrated with a thermoelectric module 26
3.3 The lightweight solar wall chimney with a thermoelectric generation module 27
3.4 The Measuring Devices 29
CHAPTER 4 EXPERIMENTAL RESULTS **33**
4.1 The roof solar concrete chimney with thermoelectric modules (RSCCT) 33
4.2 The Concrete-Based Roof Solar Chimney with Thermoelectric Generator modules and Photovoltaic (PV)-assisted ventilation (CSRCT) 38
4.3 The conventional fibre-cement roof solar concrete chimney integrated with a thermoelectric module (FSRCT) 44
4.4 The conventional lightweight solar wall chimney with a thermoelectric generation module (LSWCT) 47
CHAPTER 5 CONCLUSION AND RECOMMEDATION **50**
5.1 Conclusion 50
5.2 Recommendation 51
REFERENCES **52**
APPENDIX A **55**
VITA **57**

LIST OF TABLES

Page

Table 3-1 Materials thermal properties 21
Table 3-2 Specifications of thermoelectric MT2-1, 6-127 24

LIST OF FIGURES

Page

Figure 2-1 Heat transfer in roof 5
Figure 2-2 Schematic representation of the Roof Solar Collector 6
Figure 2-3 Typical solar chimneys used in buildings. Category 1 is the Trombe wall which includes (a), (b), and (c); Category 2 is the roof solar chimney shown in (d) and (e); and Category 3 is the combined solar chimney represented by (f) 8
Figure 2-4 Seebeck effect 11
Figure 2-5 Thermoelectric module 12
Figure 2-6 Schematic representation of heat transfer through the roof solar concrete chimney (left) and thermoelectric power generation (right) ... 12
Figure 2-7 Schematic representation of the operating principle of a concrete-based solar chimney integrated with thermoelectric generator (TEG) modules .. 13
Figure 2-8 Schematic of the thermoelectric roof solar collector (TE-RSC) 18
Figure 3-1 The houses models and south-facing roof solar concrete chimney and simple concrete roof 20
Figure 3-2 a) TEG modules integration with one module and 10 modules, matched load and electrical connection. (b). The experimental houses dimensions and positions of measurement 22
Figure 3-3 Schematic view of the south-facing concrete-based roof solar chimney integrated with thermoelectric modules (CSRCT) and a photovoltaic (PV)-assisted ventilation system, compared with a conventional concrete roof (top), dimensions of the experimental houses and locations of the measurement positions (bottom). 25
Figure 3-4 Fiber-cement solar-roof chimney combined with a thermoelectric module 26
Figure 3-5 Installation of measuring instruments inside the test house with a simple fibre-cement roof: SFR (Home 1) and a fibre-cement Solar Roof Chimney combined with a thermoelectric module (Home2) 27
Figure 3-6 Lightweight Solar Wall Chimney with a Thermoelectric Generation Module. 28
Figure 3-7 Shows the installation of measurement instruments inside a test house with a simple cement board wall (SCW; Home 1) and a lightweight solar wall chimney with a thermoelectric generation module (LSW;T: Home 2) 29

LIST OF FIGURES (CONTINUED)

Page

Figure 3-8 MS 402 EKO pyranometer 30
Figure 3-9 Hot wire anemometer 30
Figure 3-10 Datalogger “HIOKI” model LR8400-20 (±0.2s/day @23°C) 31
Figure 3-11 Heat flux (EKO) 31
Figure 4-1 Figure 4.1 Changes in indoor temperature, ambient temperature, and solar radiation intensity (2 November 2025) 33
Figure 4-2 The results of temperature changes inside the installed test house with SCR (Home 1) (November 2, 2025). 34
Figure 4-3 The results of temperature changes inside the test house with the RSCCT (Home2) on November 2, 2025. 35
Figure 4-4 Results of temperature changes inside the RSCCT (Home 2) (November 2, 2025). 36
Figure 4-5 Results of the temperature change of the ambient, the temperature difference of the thermoelectric, and the power output (Home 2), (2 November 2025) 37
Figure 4-6 Changes in indoor temperature, ambient temperature, Heat flux and solar radiation intensity (April 4, 2026) 38
Figure 4-7 Hourly variations of indoor air velocity, outlet air of the CSRCT and wind (m/s) of the two homes and the electrical power of PV panel (April 4, 2026). 39
Figure 4-8 The results of temperature changes inside the installed test house with a SCR (Home 1) (April 4, 2026) 40
Figure 4-9 The results of temperature changes inside the installed test house with CSRCT (Home2). (April 4, 2026) 41
Figure 4-10 Results of temperature changes inside the CSRCT (Home 2). (April 4, 2026) 42
Figure 4-11 Results of the temperature change of the ambient, the temperature difference of the thermoelectric, and the power output (Home 2). (April 4, 2026) 43
Figure 4-12 Changes in indoor temperature, ambient temperature, heat flux, and solar radiation intensity on June 27, 2025. 44
Figure 4-13 Results of temperature changes inside the test house with a simple fiber-cement roof: SFR (House 1), June 27, 2025 45
Figure 4-14 Results of temperature changes inside the installed test house with a Fibre-cement Solar Roof Chimney combined with a thermoelectric module (Home2), June 27, 2025. 45

LIST OF FIGURES (CONTINUED)

Page

Figure 4-15 Results of temperature changes inside the fiber-cement solar roof chimney combined with a thermoelectric module (Home 2), June 27, 2025 46
Figure 4-16 Results of temperature changes inside the fibre-cement solar roof chimney combined with a thermoelectric module (Home 2), 27 June 2025..... 46
Figure 4-17 Daily variations in ambient temperature and solar radiation intensity, as well as heat flux through the walls of the SCW and LSWCT model houses, July 25, 2025. 47
Figure 4-18 Temperature change results inside the test house equipped with a simple cement board wall (SCW; Home 2), July 25, 2025..... 48
Figure 4-19 Temperature change results inside a test house equipped with a lightweight solar wall chimney with a thermoelectric generation module (LSWCT: Home 2), July 25, 2025. 49

CHAPTER 1
INTRODUCTION

1.1 Background

Ongoing geopolitical conflicts, such as the border dispute between Thailand and Cambodia, and tensions involving major powers, such as Russia and Ukraine, have contributed to rising global fuel prices and disruptions in energy supply chains. These issues hurt economies worldwide, resulting in financial instability, decreased consumer spending, and liquidity shortages. Therefore, there is an urgent need to explore alternative energy-efficient solutions, particularly in the building sector, where the energy demand for cooling has become a significant concern.

The roof is one of the most critical components influencing the thermal performance and energy consumption of residential buildings, particularly in hot and humid tropical climates. Under intense solar radiation, a substantial portion of the incident heat is absorbed by roofing materials and transferred indoors through conduction, convection, and long-wave radiation, resulting in elevated attic and indoor air temperatures and increased cooling demand [1,2]. In urban residential housing, particularly in Southeast Asia, this heat accumulation is exacerbated by modern lightweight roofing materials and limited natural ventilation pathways, contributing to thermal discomfort, higher peak cooling loads, and increased electricity consumption from mechanical air-conditioning systems [3,4].

Thailand is a typical example of this climatic challenge. With average daytime temperatures often exceeding 32–38 °C, high relative humidity, and an annual global solar radiation of approximately 17 MJ m^{-2} day^{-1}, roofs are continuously exposed to intense solar heating throughout much of the year [5]. Previous studies have shown that the heat stored in roof tiles and decking layers is gradually transmitted into the attic space and interior ceiling, where it promotes heat buildup and reduces indoor comfort [6,7]. Conventional mitigation strategies, such as thermal insulation, radiant barriers, or reflective roof coatings, can reduce heat transfer to some extent; however, they do not fully address attic heat accumulation or airflow stagnation, particularly in low-rise residential structures [8,9].

Consequently, increasing research attention has been directed toward passive cooling strategies and ventilated roof concepts as complementary solutions to improve the thermal performance of buildings in tropical climates. Experimental and field investigations have demonstrated that ventilated roof systems, solar chimneys, and buoyancy-driven ventilation channels can enhance convective heat removal, mitigate attic temperature increases, and reduce indoor overheating without additional mechanical energy input [10–13]. Solar chimney systems, in particular, utilize solar-induced temperature gradients to generate upward airflow, thereby supporting natural ventilation and decreasing downward heat conduction through building envelopes [14,15].

In parallel, growing interest has emerged in the use of thermoelectric generators (TEGs) as a means of recovering low-grade waste heat from building envelopes. TEGs convert temperature differences directly into electrical power via the Seebeck effect and offer a compact, solid-state, and maintenance-free technology suitable for building-integrated energy harvesting [16,17]. Several studies have demonstrated the feasibility of integrating TEGs with solar-heated surfaces, glazing systems, and passive ventilation components to simultaneously support heat-mitigation functions and microscale electricity generation [18–21]. However, existing studies generally consider ventilation enhancement and thermoelectric generation as separate design strategies, and very few investigations have evaluated their combined operation within a unified roof system, particularly under real outdoor tropical conditions.

Against this background, this thesis presents extensive field investigation of concrete-based solar chimney configurations integrated with thermoelectric modules to generate electrical current using the stored heat in the roof and wall built using local commercial materials widely used for residential houses. More precisely, the aim is to experimentally examines the thermal and ventilation performance of roof and wall concrete-based solar chimney integrated with thermoelectric power generation and compare them to a conventional fiber-cement roof and wall configurations in the hot-humid climate of Thailand.

1.2 Objective

The objective of this study was to design and conduct extensive experimental investigation to explore the generation of electricity using thermoelectric modules utilizing the heat accumulated within a solar chimney of a concrete roof and a lightweight wall as the heat source.

The proposed system is designed to achieve dual functionality: (i) reducing roof and wall heat gains and enhancing buoyancy-driven airflow within the attic space and wall cavity, and (ii) harvesting supplementary electrical power from temperature gradients along the chimney channel using TEG modules.

1.3 Scopes of study

To conduct a field investigation of thermoelectric power generation using the heat of a solar chimney of a concrete roof and a lightweight wall, the following steps were undertaken:

1.3.1 Use two small houses of of 2.016 m^3 (1.2 m × 1.2 m × 1.2 m) built using fiber cement and gypsum boards for walls and concrete roof for the south facing roof (south facing LSWCT)

1.3.2 Design, build, and conduct a comparative study of the thermal performance of different configurations with the natural ventilation of a solar chimney as follows:

1.3.2.1 Concrete Roof Solar Chimney made from undulating fiber-cement panels with Thermoelectric modules (CSRCT). Two cases were considered with one

and ten modules (model MT2-1,6-127). Both natural cooling of the thermoelectric modules by the chimney induced ventilation or assisted using two small DC fans connected directly to a small Photovoltaic (PV) panel were tested.

1.3.2.2 The second considered a Lightweight Solar Wall Chimney with one thermoelectric module (LSWCT). 2.1 A configuration similar to the RSCCT acting as a thermoelectric generator (TG) was established by installing ten modules and one TE module (model MT2-1,6-127), and the performance of LSWCT with one TE module at the chimney chimney side of the concrete roof and lightweight wall natural ventilation of solar chimney (RSCCT) and (LSWCT) was compared with that of SCR and SCW.

1.3.3 Thermal performances are compared to a Simple fiber-cement Roof (SFR) and a Simple Cement Wall (SCW) configuration respectively.

1.3.4 Assess the electricity generation of thermoelectric modules for the different configurations considered.

The tests were conducted for several days under different ambient conditions. The experimental small houses were located in Krabang District, Bangkok 10520, Thailand. For each series of configurations, tests were performed on the same day and time under the same environmental conditions and using the same measurement equipment and devices.

1.4 Expected outcome

The expected benefit is to gain a good understanding of thermoelectric power generation using the solar chimney heat of a concrete roof and lightweight wall to provide guidelines and new alternatives for concrete roof and lightweight wall developers and users, and to offer valuable recommendations and suggestions for application and integration in residences, homes, and buildings.

The contributions of this study are threefold. First, it provides empirical evidence demonstrating how a concrete-based based roof and lightweight wall chimney configuration can simultaneously mitigate heat gain and improve natural ventilation in a realistic outdoor tropical environment. Second, it presents one of the few experimental assessments that integrates thermoelectric energy harvesting directly into a ventilated roof system, enabling co-benefits from the same thermal gradient that drives the buoyancy airflow. Third, the study offers performance insights and design implications that support the development of hybrid passive–active roof and wall technologies for energy-efficient residential buildings in tropical and subtropical regions.

CHAPTER 2
LITERATURE REVIEW AND THEORETICAL CONSIDERATION

2.1 Climate and thermal challenges in tropical housing

In Thailand, as in many other tropical regions, residential buildings are increasingly featuring modern roof designs that are both visually appealing and cost-effective. Common roof types in housing estates include hips, triangular gables, and square or curved roofs. Although these designs effectively protect against rain and shield against direct short-wave solar radiation during the day, they are inadequate for mitigating long-wave radiation. Consequently, solar heat is absorbed by the roof surface and transferred indoors via conduction, convection, and radiation. This process increases indoor temperatures above ambient levels, thereby forcing air-conditioning systems to work harder, which in turn increases electricity consumption and household energy costs.

Conventional roofing and wall systems often prioritize aesthetic appeal over thermal performance. The most common roof and wall designs–gable, triangular gable, and flat/curved forms—fail to effectively block longwave radiation, resulting in heat transfer into living spaces through conduction and re-radiation. These inadequacies underscore the importance of integrating passive cooling technologies and energy-efficient design principles in tropical residential construction.

2.2 Thermal insulation and radiant barriers in roofing

Solar radiation primarily comprises short-wave energy that is absorbed upon contact with the surface of the roof tiles, resulting in an increase in the temperature of the material. A portion of the accumulated heat is dissipated to the external environment via convection and longwave thermal radiation. The remaining heat is retained within the roofing materials and subsequently transferred to the attic space. Heat propagation occurs via radiative and convective mechanisms within this zone. The radiant heat that reaches the upper surface of the ceiling slab is absorbed, causing an increase in the surface temperature, which in turn facilitates further heat transfer into the indoor environment. The cumulative process of the thermal exchange through the roof structure is illustrated in Figure 2-1

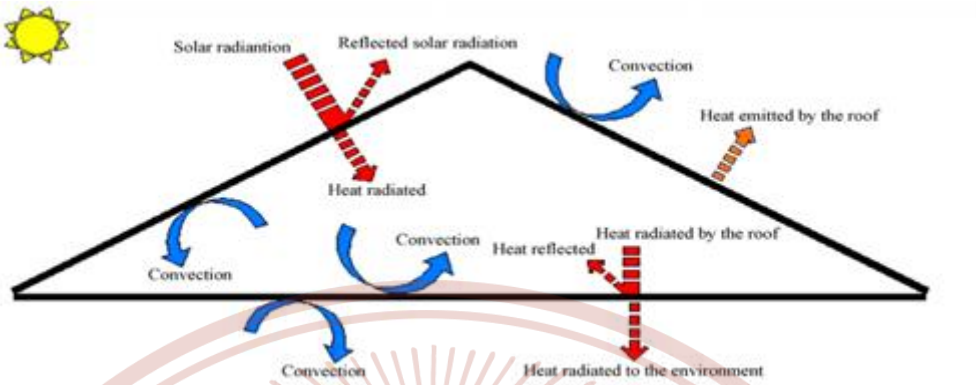


Figure 2-1 Heat transfer in roof

Roofing materials and surface treatments significantly influence heat gain through the roof envelope. Michels et al. studied the application of radiant barriers in clay tile roofs and demonstrated up to a 30% reduction in heat flux. Similarly, Levinson et al. explored the impact of cool-colored roof coatings with high near-infrared reflectance, offering a practical approach to reduce solar absorption in tropical regions. These strategies are often applied independently of passive ventilation systems, suggesting a gap in roof-integrated solutions.

2.3 Passive cooling and natural ventilation techniques

The roof is the primary envelope through which solar heat is transmitted indoors; thus, its design strongly influences building thermal performance. Conventional roof forms, such as gables, triangular gables, and flat or curved roofs, prioritize aesthetic appeal but often fail to mitigate longwave radiation effectively.

Passive ventilation has been extensively studied as a low-cost and energy-saving alternative to active cooling methods. Solar chimneys are particularly effective in promoting air circulation by using the buoyancy of heated air to induce vertical airflow and extract hot indoor air. Early work by Khedari et al. demonstrated the effectiveness of roof-integrated solar collectors in enhancing natural ventilation and reducing indoor heat buildup in tropical housing.

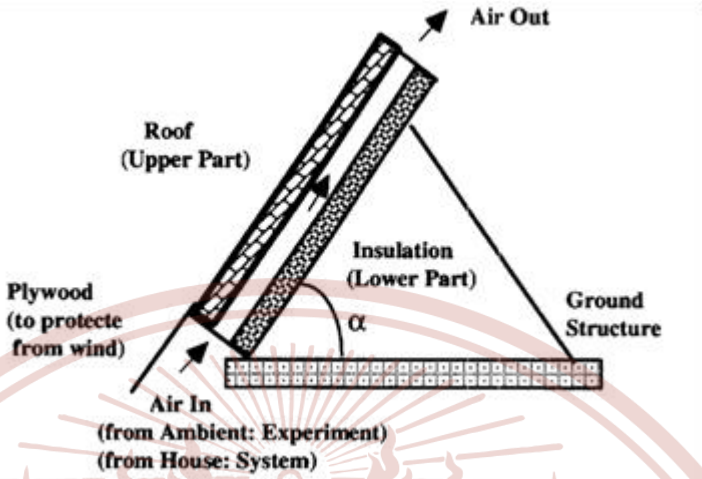


Figure 2-2 Schematic representation of the Roof Solar Collector

Further investigations by Waewsak et al. and Amornleetrakul et al. focused on bioclimatic and ventilated roof tiles, showing notable improvements in air movement and temperature control. In parallel, DC fan-assisted ventilation systems have also been evaluated as a hybrid approach for increasing air circulation and reducing attic temperatures. Despite their effectiveness, these solutions often lack integration with energy-harvesting systems, thereby limiting their overall sustainability potential.

2.4 Solar chimney designs

2.4.1 Principle of solar chimney

Solar chimneys represent an effective and low-cost bioclimatic design strategy for minimizing energy consumption in buildings. By harnessing solar radiation to induce thermal buoyancy, these systems enhance natural ventilation rates, thereby reducing the dependence on mechanical cooling and heating systems and contributing to a reduction in the associated carbon dioxide (CO2) emissions. Depending on the architectural context, solar chimneys may be integrated into vertical facades (e.g., Trombe walls) or roof structures (e.g., roof-mounted solar collectors). Their overall performance is influenced by several key parameters, including geometric configuration, tilt angle, material thermal properties, and prevailing climatic conditions. The optimal design and integration of these systems can lead to significant improvements in thermal comfort and energy efficiency in residential and commercial buildings.

Solar chimneys, which can be oriented vertically or inclined, are categorized into two principal configurations: wall-mounted solar collectors (such as Trombe walls) and roof-integrated solar collectors. Structurally, a typical solar chimney comprises three primary elements: an absorber surface, an intermediate air gap, and a transparent glass cover with high solar transmittance. This configuration was engineered to harness the maximum solar energy to enhance the stack effect, thereby

promoting natural airflow. In certain implementations, the glass cover may be replaced with an opaque panel or integrated with photovoltaic (PV) modules to generate electricity, in addition to facilitating ventilation.2.4.2 Type of solar chimney

A solar chimney is a passive solar strategy for enhancing natural ventilation in buildings. The fundamental principle underlying its operation is thermal buoyancy, which is induced by variations in air density resulting from temperature gradients between the indoor space and the chimney cavity. As solar radiation heats the chimney, the air within the cavity becomes less dense and rises, thereby creating a pressure differential that drives airflow from the interior of the building through the chimney, facilitating continuous natural ventilation. Figure 2.3 shows the primary configurations of solar chimneys commonly implemented in buildings. Note that the figure excludes solar chimneys integrated with other hybrid systems. Based on their installation location and structural configuration, solar chimneys can generally be classified into three main categories: (1) Trombe walls, which are integrated into vertical building facades; (2) roof-mounted solar chimneys, which utilize inclined or horizontal surfaces; and (3) combined solar chimneys, which incorporate elements of both wall- and roof-based systems, or integrate with fenestration components such as windows.

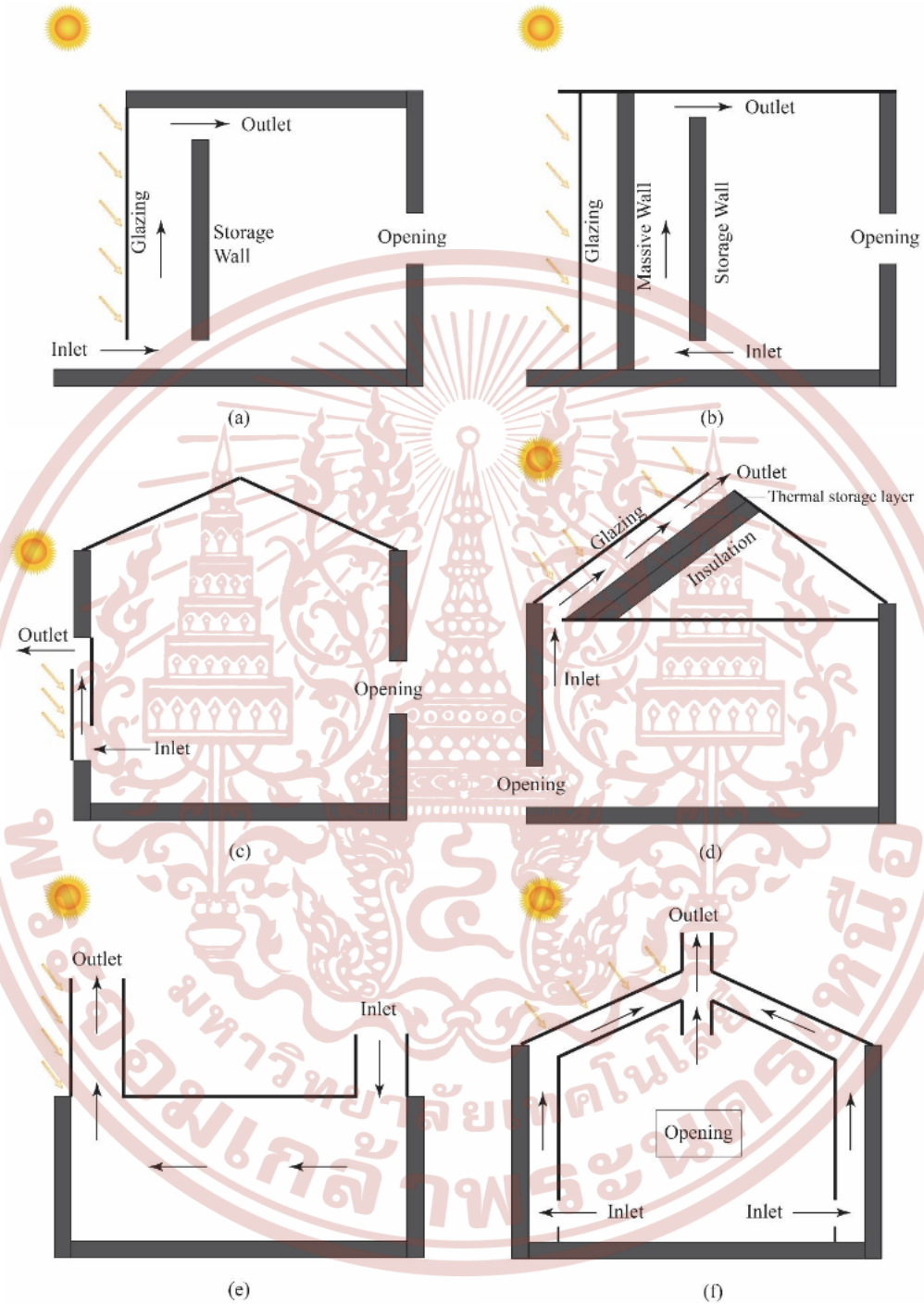


Figure 2-3 Typical solar chimneys used in buildings. Category 1 is the Trombe wall which includes (a), (b), and (c); Category 2 is the roof solar chimney shown in (d) and (e); and Category 3 is the combined solar chimney represented by (f)

Figure 1(a) shows a schematic representation of the Trombe wall system (Category 1), which is typically employed for passive winter heating. This configuration consisted of an external glazing layer and interior thermal mass wall. Transparent glazing permits solar radiation to penetrate the cavity, thereby warming the enclosed air. Owing to the resulting temperature gradient, the thermal buoyancy induces an upward airflow within the cavity. The heated air is then directed into the interior space through the top outlet, whereas the lower-left opening facilitates air exchange with the outdoor environment. Conversely, the bottom-right opening allows for air circulation from the indoor space.

During summer, the Trombe wall can be adapted for passive cooling by altering the positions of the inlet and outlet openings, similar to the configuration depicted in Figure 1(c), to allow hot indoor air to be expelled outdoors through the chimney effect. The contemporary enhancement of the traditional Trombe wall involves the integration of phase-change materials (PCMs) into the thermal storage wall. These materials absorb latent heat during phase transitions, enabling more compact and lightweight thermal storage than conventional high-mass walls.

A composite Trombe–Michel wall was also developed based on a Trombe wall, as shown in Figure 1(b). It was designed to overcome heat losses from the interior room. Owing to its structure, it can only be applied for winter cooling. One of its disadvantages is that it cools the building when it actually needs to heat it up at night or during winter when the storage wall becomes colder than the indoor air. To overcome this disadvantage, relevant materials, such as PCMs, can be used to retain heat for later use during non-sunny days, winter, or at night. In contrast to the Trombe wall, the movable air in the chimney cavity is not heated by direct solar radiation; however, convection occurs between the internal air and the massive wall.

As depicted in Figure 1(c), a glazed solar-chimney wall presents a viable passive cooling strategy for tropical climates. This system consists of double-glazed panels enclosing an air cavity with strategically placed openings: one at the bottom of the room-facing panel and another at the top of the ambient-facing panel. Functionally similar to a Trombe wall, a glazed solar-chimney wall promotes natural ventilation by inducing air circulation through thermal buoyancy. Experimental studies have demonstrated the effectiveness of glass facades in reducing the heat gain in residential structures located in hot and humid regions, thereby enhancing thermal comfort and reducing reliance on mechanical cooling systems. However, the performance of a chimney is highly dependent on its geometric parameters, particularly height and width. In climates where solar intensity or space constraints limit the optimal sizing of the structure, its efficiency may be significantly reduced.

Figure 1(d) presents a typical roof-mounted solar chimney (Category 2), a passive ventilation strategy that harnesses solar energy to enhance airflow through thermal buoyancy. Given that the efficiency of solar chimneys is largely governed by the temperature differential between indoor and cavity air, a solar air collector was

integrated into the roof to intensify this thermal gradient. An external glazing layer facilitates solar radiation absorption, thereby heating the air within the cavity. Beneath this cavity, a thermal storage layer was incorporated to prolong heat availability, thereby enabling the system to function during periods of low solar insolation, such as cloudy days or at night. To minimize thermal losses, an insulation layer was positioned beneath the storage mass. This type of roof solar chimney can be configured as either inclined (as shown in figure 1(d)) or vertical (figure. 1(e)), depending on architectural and functional requirements. Compared to Trombe wall systems, airflow within roof solar chimneys may experience increased resistance owing to the presence of duct bends, potentially affecting overall ventilation performance.

Figure 1(e) presents a vertical roof-mounted solar-chimney configuration that distinguishes itself from conventional designs by incorporating an additional vertical shaft that functions as an air inlet. This system utilizes two separate chimneys integrated into the roof structure; one acts as a solar collector to absorb solar radiation and generate buoyancy-driven airflow, whereas the other serves as an air inlet through which fresh air is drawn into the building. Alternatively, the air inlet may take the form of conventional architectural openings, such as windows or doors, located on the opposite side of the space. This dual-chimney configuration can be advantageous in specific applications where spatial or functional constraints necessitate vertically oriented ventilation pathways. However, a primary challenge associated with this design is the potential for short-circuited airflow, in which both the inlet and outlet are positioned at similar elevations. This configuration can lead to limited air circulation or partial ventilation confined to the upper portions of the room, thereby reducing the overall effectiveness of the system in promoting full-room air exchange.

Figure 1(f) presents a combined solar chimney system classified under Category 3, which integrates both vertical and roof-mounted components to enhance the performance of natural ventilation. In this design, a vertical solar collector is installed above the roof level, and air ducts are distributed along both the building façade and roof structure to facilitate the airflow. Indoor air can be exhausted to the exterior either directly through the vertical collector or indirectly via the duct system, which channels it toward the collector. Fresh outdoor air was introduced through a designated opening located on the side wall, as depicted in the center of the schematic. The effectiveness of the system is primarily governed by the temperature differential generated within the vertical solar collector, which is influenced by factors such as the collector height, surface area, and thermal properties of construction materials. Similar to other roof-based solar chimney configurations, one of the persistent challenges is minimizing airflow resistance, particularly that caused by bends in the ductwork, which can significantly impede buoyancy-driven ventilation.

2.5 Thermoelectric modules in building applications

Thermoelectric (TE) modules, which convert thermal gradients into electricity via the Seebeck effect, have recently been explored for building-integrated applications. Although commonly used in niche electronic cooling or waste heat recovery, TE modules, such as MT2-16-127, have the potential for low-power generation from solar-induced heat differentials. Integrating TE modules into passive roof systems can enable simultaneous cooling and micropower generation, thereby enhancing energy efficiency.

Ogoli demonstrated that buildings with high thermal masses experience substantial internal heat buildup, which can be partially offset by active heat removal or conversion technologies [17]. However, few studies have combined thermoelectric generation with skylight and ventilation systems, particularly under real tropical climatic conditions.

2.5.1 Principle of thermoelectric [17]

The foundational principle behind thermoelectric energy generation is rooted in the Seebeck effect, discovered by German physicist Thomas Johann Seebeck. Seebeck observed that when two dissimilar conductive materials are joined at two junctions and subjected to a temperature gradient, an electromotive force (EMF) is generated, which causes an electric current to flow through a closed circuit. This phenomenon occurs because of the difference in charge carrier diffusion rates at the hot and cold junctions, resulting in voltage generation across the material. The Seebeck effect is fundamental to thermoelectric devices and is shown in Figure 2-4

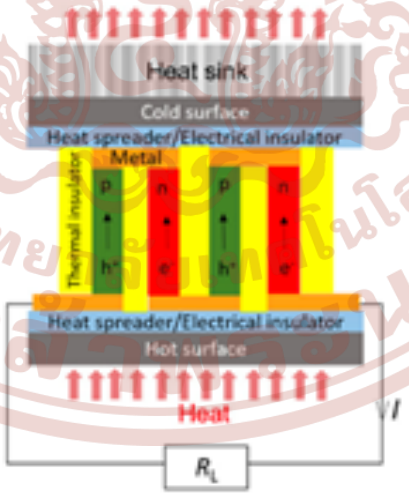


Figure 2-4 Seebeck effect

Based Based on the foundational principle of the Seebeck effect, this concept has evolved into TE devices that convert a temperature gradient into electrical energy. These devices operate on the principle of direct energy conversion, where heat is

applied to one side and cooling is applied to the opposite side of the device establishes a thermal gradient, generating voltage and current in a closed circuit.

A typical thermoelectric module comprises semiconductor materials arranged in both n-type and p-type junctions, which are electrically connected in series and thermally connected in parallel, as shown in Figures 2.5 and 2.6. When a load is connected across the device, the circuit is completed, and electrical power is generated owing to the temperature differential.

Thermoelectric modules are versatile and can function in two ways.

As a power generator, when exposed to a temperature difference, it produces electrical power from heat. Thermoelectric cooler (TEC): When supplied with direct current (DC), it acts as a solid-state heat pump, absorbing heat from one side and rejecting it from the other. To enhance the thermal transfer efficiency, heat exchangers or heat sinks are often integrated on both sides of the TE module to improve heat absorption and dissipation, heat transfer through the roof and wall of the solar concrete chimney, and thermoelectric power generation.

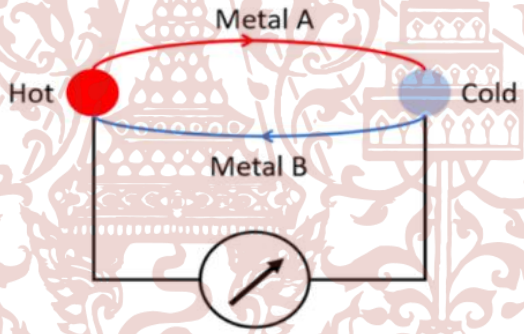


Figure 2-5 Thermoelectric module

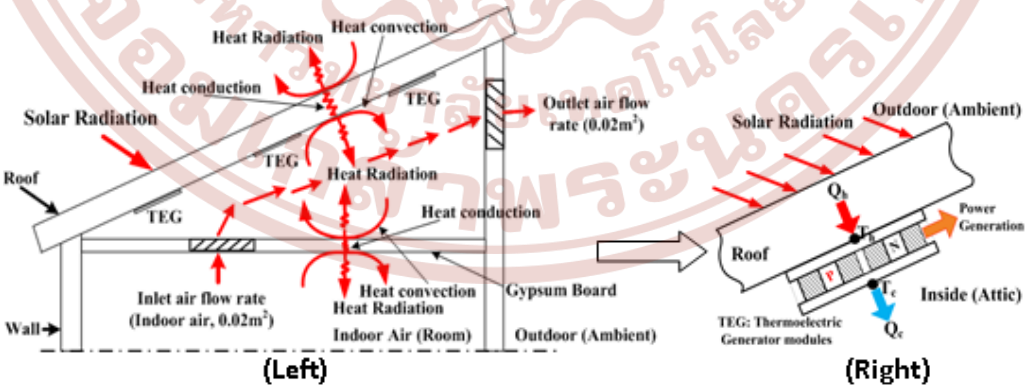


Figure 2-6 Schematic representation of heat transfer through the roof solar concrete chimney (left) and thermoelectric power generation (right)

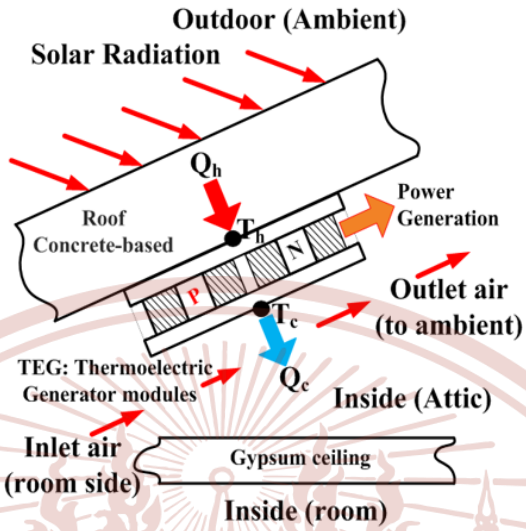


Figure 2-7 Schematic representation of the operating principle of a concrete-based solar chimney integrated with thermoelectric generator (TEG) modules

Solar radiation incident on the concrete roof is partially reflected and partially absorbed by the roof surface (figures 2.6 and 2.7). A fraction of the absorbed energy is lost to the ambient environment through convection and long-wave radiation, whereas the remaining energy is stored within the concrete mass and transferred by conduction through the roof thickness. The conducted heat increases the attic air temperature, creating a temperature-dependent density difference between the attic and the outdoor environment. This density gradient generates buoyancy-driven airflow, causing warm air to ascend and exit through the solar chimney outlet. The resulting pressure difference induces the inflow of cooler replacement air through ceiling ventilation openings. The result is a steady natural ventilation loop: indoor air circulates more, less heat accumulates in the building, and thermal comfort goes up. The thermoelectric generator (TEG) modules are integrated with the concrete roof ventilation structure to exploit the temperature gradient generated by solar heating. The hot side of the TEG modules is thermally coupled to the inner surface of the concrete roof, where heat absorbed from incident solar radiation is transferred and stored within the concrete mass. The cold side, meanwhile, faces the cooler attic airflow. As the attic air is heated, its density decreases, inducing buoyancy-driven natural ventilation. The resulting upward airflow transports heated air toward the roof outlet and exhausts it to the ambient environment, while simultaneously enhancing convective heat dissipation from the cold side of the TEG modules. A persistent temperature difference therefore exists across the thermoelectric elements, and they convert that thermal gradient into electricity through the Seebeck effect. This discussion applies to wall solar chimney configuration as well creating an ascendent vertical upward air flow.

2.6 Literature Review

Researchers have considered and developed many ways to slow heat transfer through building envelopes and bring down cooling loads. A separate line of work, driven by the push for energy sustainability, has explored recovering the waste heat that buildings absorb. Thermoelectric generators (TEGs) fit both goals: they turn a temperature difference directly into electricity through the Seebeck effect, so they can pull useful power out of a hot roof while the cooling system removes heat. Several groups have combined passive cooling with TEG harvesting to lower electricity use and generate small amounts of renewable power from the heat that roofs store [29]. To overcome this problem, various research studies were reported, and an important variety of solutions and alternatives are proposed to reduce the heat entering the house, saving energy from the widespread use of air conditioners both domestically and internationally.

Khedari et al. [10] discussed the possibility of offering thermal comfort in new housing built in European style and situated in a hot and humid climate, without inducing mechanical energy cost, by means of a constructive element: the Roof Solar Collector (RSC). possible, on the one hand, to minimize the fraction of the solar flux absorbed by the dwelling (insulation). With this RSC it is and, on the other hand, to induce a natural ventilation which improves its thermal comfort. The influence of length and tilt angle of the RSC and local constructing materials used on the performance of the RSC is studied experimentally. The results of the study were that the appropriate materials of the roof solar collector, with regard to the improved natural ventilation, should be CPAC Monier concrete tiles on the outer side and gypsum board on the inner one. The optimum length of roof solar collector must be shorter on the order of 100 cm and tilted at 30”. The induced natural ventilation rate was about 0.08-0.15 $m^3.s^{-1}.m^{-1}$.

Waewsak et al. [11] reported an innovative configuration of bioclimatic developed by the building scientific research center (BSRC-BCR) that functions to decrease daily heat gain through the roof fabrics, to induce significant air ventilation rate, which improves the thermal comfort of residents, to ensure appropriate daylighting without any overheating and to act as a roof radiator during nighttime. The BSRC-BCR is composed of a combination of CPAC Monier concrete and transparent acrylic tiles on the outer side, air gap and another combination of gypsum with an aluminum foil board and translucent sheets on the room side. The experimental results show that the BSRC-BCR is extremely interesting as it can reduce roof heat gain significantly, provide sufficient natural lighting for housing and induce high air change that improve indoor thermal comfort. The temperature difference index TD of BCR was always lower or close to neutral than that of RSC during the hottest period of the day. The indoor illuminance delivered by the BSRC-BCR was about 300 and 140 lx in summer and winter, respectively. The ACH was about 13–14 and 5–7 in summer and winter, respectively, two times that induced by the RSC.

Chungloo, et al. [12] study aimed to experimentally investigate a solar chimney that integrates the cool air above the moist earth with the warm air in the chimney to enhance heat protection of a building. The exterior surface of a testing chimney exposed to the simulated moderate and high solar intensity of 10-700 W/m2 and 80-980 W/m2 gives a surface temperature of 30.2-63.2°C. Cool air of 26.0-27.8°C entering the high mass solar chimney reduces the surface temperature of the internal wall by 2.1-16.9°C with delay time of 1-3 hours compared to the exterior wall's temperature. The air temperature at the outflow is higher than that of the inflow by 10°C at 6:00 p.m. , corresponding to the highest air ventilation rate. With similar values of air temperature in the chimney, the surface temperatures with moving air are found to be less than that of the computed stationary air by 8.5-8.9°C during the nighttime. Therefore, the proposed solar chimney performs as an active insulator for both daytime and nighttime. The coefficient of discharge of 0.42-0.67 are derived from the relationships between the values of air velocity and the outflow-inflow temperature differences.

Amornleetraku, et al. [13] investigated the thermal performances and heat gain reduction of a new roof tile design referred as Ventilated Roof Tile (VRT) compared with an ordinary corrugated concrete roof tiles (CCR). The outside dimension of each small house was 1.70 x 1.70 x 2.85 m3 (W x L x H) and inside dimension was 1.50 x 1.50 x 2.20 m3. The volume of each room was 4.95 m3. The gable roofs slope was 25o and surface area of VRT was 2.58 m2 per each side facing north and south. The VRT tile composed of upper cement plate 40 × 40 cm2 and lower cement plate 30 x 40 cm2. Between plates was 3 cm thickness air gap. The experimental results showed that the top surface of VRT was lower than CCR about 2.10oC for average temperature (from 6:00 – 18:00) and made VRT room temperature lower than CCR about 1.41oC for average temperature. VRT could reduce heat gain with air flow rate through the roof tiles gaps varied following the solar radiation, during time 8:00-17:00 the natural ventilation varied from 0.003-0.014 m3/s (10.6-50.0 m3/hr.). Observed that, during 17:00-18:00, the air flow rate is about 0.003 m3/s (10.8 m3/hr.) due to heat accumulated in the attic space and roof tiles.

Bansal et al. [14] reported a steady state mathematical model developed for a solar chimney which is used to describe the effect of thermally induced ventilation in buildings. The model takes into consideration different sizes of the openings of a solar chimney with varying values of the discharge coefficients. Numerical calculations performed for different values of ambient temperature and solar radiation show that a solar collector area of 2.25 (m^2) is able to induce an air flow between 140 (m^3/hr) to 330 (m^3/hr) for solar radiation of 200 (W/m^2) and 1000 (W/m^2) respectively.

Passive ventilation systems are being increasingly proposed as an alternate to mechanical ventilation systems because of their potential benefits in terms of operational cost, energy requirement and carbon dioxide emission [15]. Solar chimney is an excellent passive ventilation system which relies on natural driving force, that is,

the energy from the sun. They showed that a significant amount of research works has been done on solar chimney since the 1990s. Authors presented an overview of solar chimney research that has taken place in the last two decades. The review focuses on two main areas of research –the effects of geometry and inclination angle on the ventilation performance of a solar chimney. The experimental investigations of solar chimney have dominated the existing literature. However, numerical modeling of solar chimney using computational fluid dynamics (CFD) technique has attracted increasing attention. Moreover, this review found that solar chimney as a passive ventilation strategy has not been fully understood.

Rowe [16] explained that a thermoelectric generator is a unique heat engine in which charge carriers serve as the working fluid. It has no moving parts, is silent in operation and very reliable. However, its relatively low efficiency (typically around 5%) has restricted its use to specialised medical, military and space applications where cost is not a main consideration. During the past 10 years thermoelectrics has attracted increasing attention as a 'green' and flexible source of electricity able to meet a wide range of power requirements. Relatively recently it has been realized that in situations where the supply of heat is cheap or free, as in the case of waste heat, efficiency of the conversion system is not an overriding consideration. The use of waste heat as an energy source particularly at temperatures below 140C substantially increase the commercial competitiveness of this method of generating electrical power. The results of a recent investigation of the performance of thermoelectric generating systems powered by waste hot water indicate that, over a three year operating period, electrical power can be produced by this method and at a price which matches that of conventional utilities. This paper provides an overview of environmentally friendly applications of thermoelectric generation and assess its potential as an alternative source of electrical power

Disalvo [17], showed that in a typical thermoelectric device, a junction is formed from two different conducting materials, one containing positive charge carriers (holes) and the other negative charge carriers (electrons). When an electric current is passed in the appropriate direction through the junction, both types of charge carriers move away from the junction and convey heat away, thus cooling the junction. Similarly, a heat source at the junction causes carriers to flow away from the junction, making an electrical generator. Such devices have the advantage of containing no moving parts, but low efficiencies have limited their use to specialty applications, such as cooling laser diodes. The principles of thermoelectric devices are reviewed and strategies for increasing the efficiency of novel materials are explored. Improved materials would not only help to cool advanced electronics but could also provide energy benefits in refrigeration and when using waste heat to generate electrical power.

Köysal, et al. [19] work concerned an experimental design for generating power from thermoelectric generator (TEG) and linear Fresnel lens collector with one-axis solar tracking system. Main purpose of this experimental design is to measure the performance of the TEG with linear Fresnel lens collector. This work also aimed to create a mathematical model by using adaptive neuro fuzzy inference system (ANFIS) model so that the electrical production estimates of the constructed system can be made for a given data set. For this reason, two individual systems, selective surface adapted for achieving medium temperature scale and nonselective surface for low temperatures, were constructed. There are two different coolant systems, which are passive and active, to create effective open circuit voltage values. Experimental results show that the maximum open circuit voltages were obtained as 0.442 V and 1.413 V for experimental system with selective surface adapted, as 0.341 V and 0.942 V with nonselective surface adapted when the received radiated power on Fresnel lens was measured nearly 625 W/m^2 on average in the noon time. The collected data such as solar irradiation, wind speed, ambiance temperature, and open circuit voltage were used for (ANFIS) modeling. Obtained result collected in Samsun/Turkey shows that experimental calculations and modeling are consistent with each other.

Thanthong, et al. [20] proposed a new concept of waste heat thermoelectric power generation using radiative heat transfer with horizontal finned heat absorber (TEG-RFA). To this end, a lab-scale experimental setup was built using a heated plate, horizontal finned absorber, thermoelectric modules and air-cooled heat sink. The dimensions of heated plate were 297 mm length 182 mm width. Four sets of horizontal finned absorber 41 mm wide and 55 mm length with 40 x 40 mm thermoelectric module were assembled to absorb the radiative heat emitted by the heated plate. At the back side, a finned aluminum heat sink 119 mm wide and 200 mm length with two DC fans was installed to cool the 4 sets of TEG. The absorber assembly was well insulated on the four lateral sides to protect heat transfer to the cooling heat sink. Five air gap space between the heated plate and finned absorber (1, 2, 3, 4 and 5 cm) and five electrical powers (1000, 1100, 1200, 1300 and 1400 watts) supplied to the heater were considered. Temperatures at different positions and generated voltage and current were recorded. Experimental results showed that the electrical current generated increased with increasing the power supplied to the heated plate and decreased when increasing air gap space. Under the test conditions considered, the maximum electrical power generated and the corresponding temperature difference between the hot and cool sides of thermoelectric modules were 1.20 Watt and 118C at 1400 Watt and 1 cm air gap whereas the minimum measured parameters were 0.060 Watt and 14.90C at 1000 Watt and 5 cm air gap. Therefore, they demonstrated that this concept of thermoelectric generator with horizontal finned absorber cooled using air is an interesting alternative for waste heat recovery namely in industries.

Chantawong P. [28] recent study has extended roof-based passive cooling systems by combining solar-assisted ventilation of a lightweight roof chimney (LRC) integrated

with DC fans as a method for reducing roof heat gain and improving indoor ventilation in hot and humid climates. The system consisted of a double-layer roof assembly with clear polycarbonate as the outer roof, gypsum board as the ceiling layer, and openings at the bottom and top to support airflow. Two DC fans powered by solar energy were used to exhaust hot air from the attic and indoor space, thereby strengthening air circulation and reducing heat accumulation beneath the roof.

The experimental results showed that the house equipped with the LRC and DC fans performed better than the house with a simple lightweight roof. Indoor air temperature in the LRC house was about 0.5-2°C lower during the daytime, while attic temperature was also lower than that of the reference house. In addition, the indoor air velocity in the ventilated house was substantially higher, reaching about 0.01-0.92 m/s, compared with only 0.01-0.024 m/s in the house with the simple lightweight roof. These results indicate that the addition of solar-powered fans can significantly improve air movement and ventilation effectiveness within the building.

Maneewan et al. [29] investigated a thermoelectric roof solar collector (TE-RSC) designed to reduce attic heat gain while simultaneously generating electricity to operate a ventilation fan. The system combined a transparent glass cover, an air gap, a copper absorber plate, thermoelectric modules, and a finned heat sink integrated into a conventional roof solar collector structure, figure 2-8

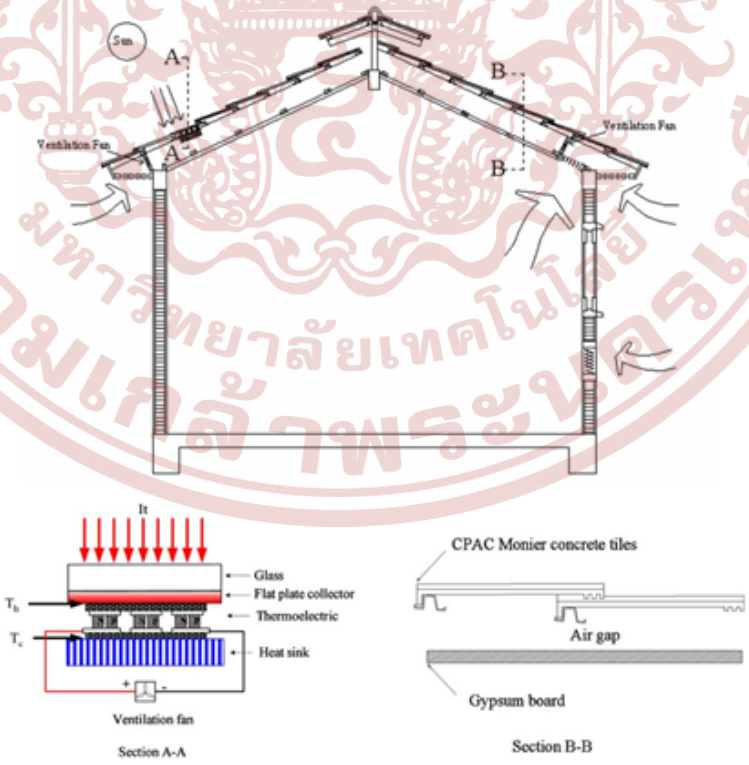


Figure 2-8 Schematic of the thermoelectric roof solar collector (TE-RSC)

Numerical simulation using TRNSYS showed that the TE-RSC could generate about 9 W under solar radiation of approximately 972 W/m² and an ambient temperature of 35°C. The induced attic ventilation rate was significant, reaching about 20-45 air changes per hour (ACH), depending on solar intensity and season. The system reduced ceiling heat transfer compared with a conventional non-insulated house, with ceiling heat gain reduction reported in the range of about 25-35%. The corresponding cooling load reduction was about 375 W in summer and 180 W in winter, indicating that the system could contribute meaningfully to reducing indoor cooling demand.



CHAPTER 3
EXPERIMENTAL SETUP AND METHODOLOGY

Let remind that the objective of this thesis is to develop and conducted detailed field investigation of thermoelectric power generation using the attic heat of a roof solar concrete chimney and lightweight solar wall chimney, which are widely used for low-cost residential houses under hot and humid climate conditions in Thailand.

3.1 The roof solar concrete chimney integrated with thermoelectric modules

3.1.1 Experimental setup and test houses

The two small experimental houses were located in the Krabang District, Bangkok 10520, Thailand. The experiment was conducted using two identical model houses of 2.016 m^3 volume and were oriented southward to maximize solar exposure under tropical daytime conditions. The design followed laboratory and field testing practices reported in prior studies [29]. The walls were constructed from 8-mm plasterboard finished with white paint to enhance reflectivity, while the ceiling consisted of 6-mm plasterboard. Each roof employed pearl-blue fiber-cement tiles installed at a 30° slope, providing an approximate roof surface area of 2.04 m^2. The overall layout of the houses and the south facing roofs is showen in figure 3-1



Figure 3-1 The houses models and south-facing roof solar concrete chimney and simple concrete roof

The first model house served as the reference configuration and was fitted with a conventional simple fiber-cement roof (SCR). The second house incorporated a roof solar–concrete chimney with thermoelectric modules (RSCCT). In this configuration, the roof assembly consisted of a two-layer structure: an outer layer of double-corrugated fiber-cement tiles to promote air passage and an inner flat fiber-cement layer approximately 8 mm thick. The two layers were separated by a 0.01m ventilation channel, forming the solar chimney passage. Openings with an area of approximately 0.02 m^2 were provided at both the inlet (ceiling level) and outlet (ridge level) to induce buoyancy-driven airflow under heated conditions. A plastic access door (0.6 m^2, 7.5 cm thickness) and a 0.4-m^2 louvre were installed on the north façade to allow air exchange. The thermophysical properties of construction materials used are given in Table 3-1

Table 3-1 Materials thermal properties

Type of material	Fibre-cement board	Thermal insulation
Thermal conductivity (W/m.K)	0.297	0.029
Density (kg/m^3)	775	120
Specific heat capacity (J/kg.K)	1.09	840
Emissivity	0.95	0.9

3.1.2 Thermoelectric modules integration

To enable simultaneous passive cooling and low-grade heat energy recovery, TE module can be installed at the rear side of roof. Figure 3.2 shows schematic for one and ten TEG modules (model MT2-1, 6-127; 40 mm × 40 mm) installed along the RSCCT channel, as illustrated in Figure 3.2(a)–(b). The modules were positioned at locations with the maximum expected temperature gradient between the heated roof surface and the cooler interior layer. The key specifications of the TEG devices, including thermal conductivity, maximum operating temperature, and material geometry, are summarized in Table 2 [20–23].

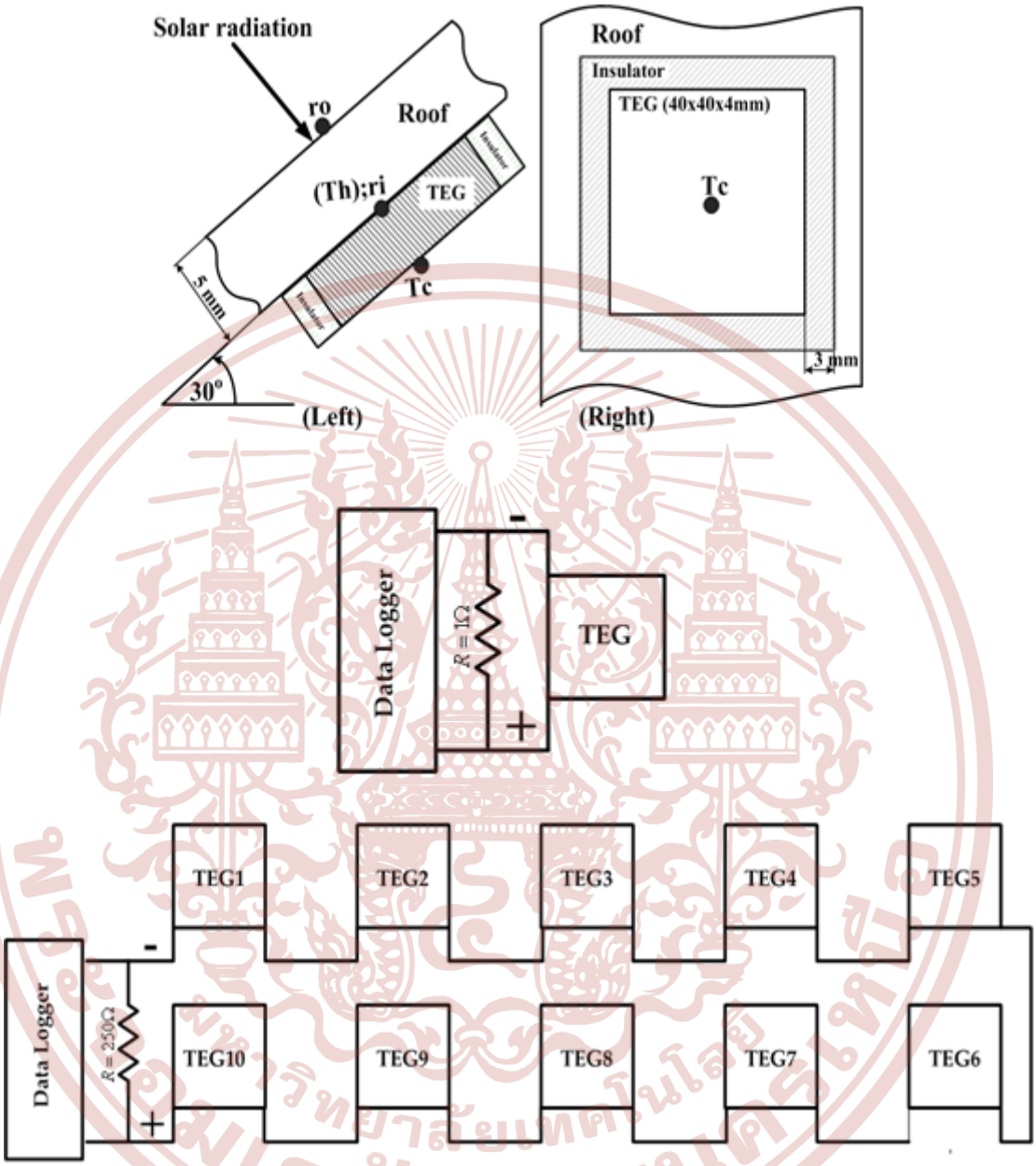


Figure 3-2 a) TEG modules integration with one module and 10 modules, matched load and electrical connection.

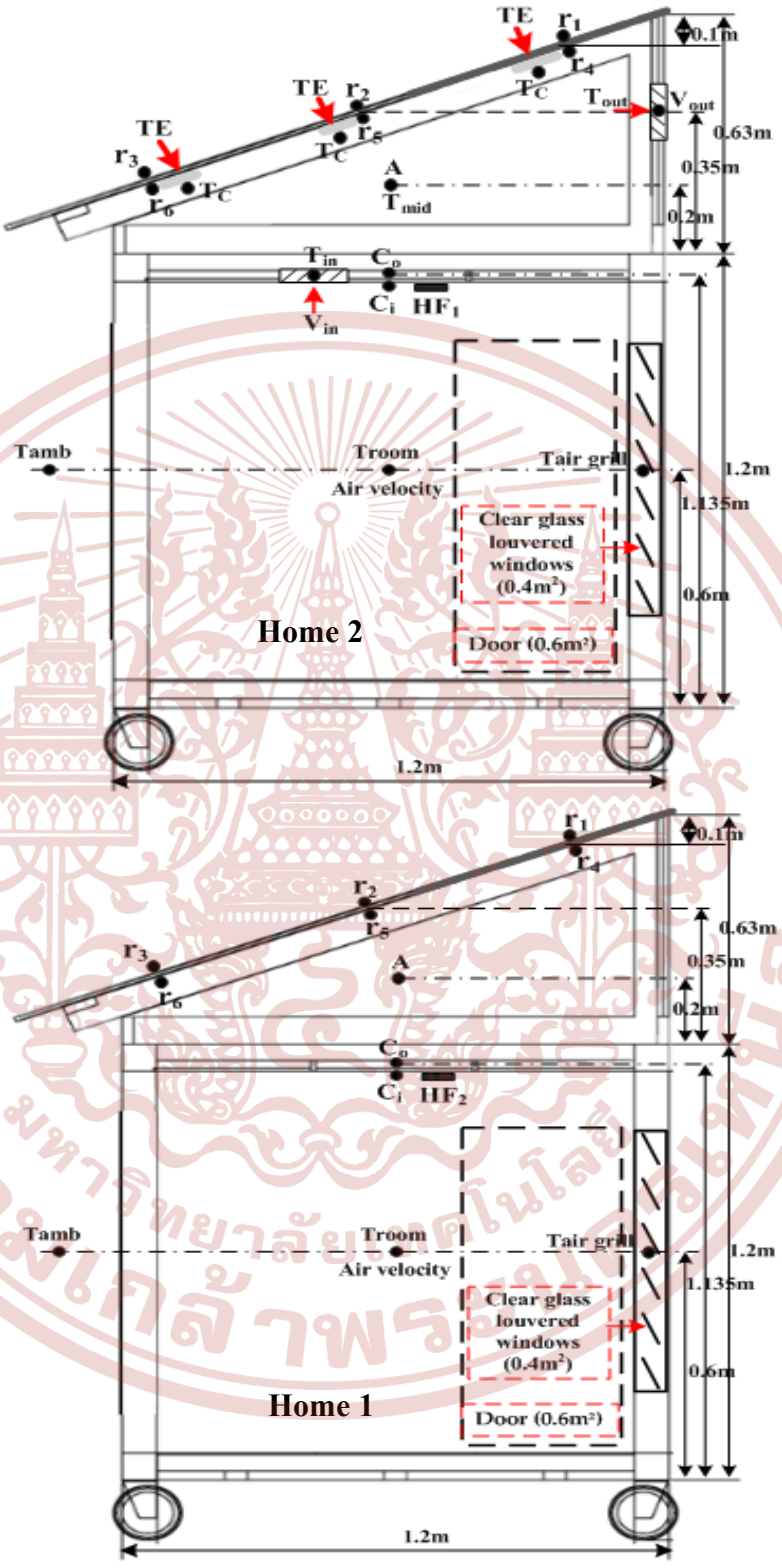


Figure 3-2 (b) The experimental houses dimensions and positions of measurement.

The electrical output was routed through 20-AWG UL1007 insulated wiring rated at 80°C and 300 V and connected to a matched resistive load of 250 Ω (Figure 3.1(b)). The output voltage was recorded for subsequent power calculations based on Ohm's law. This configuration ensured stable operation without an external power supply and enabled the evaluation of the energy-harvesting potential under natural environmental conditions.

Table 3-2 Specifications of thermoelectric MT2-1, 6-127

Leg height (mm)	1.5
Area of the thermoelement (mm²)	1.96
Contact height (mm)	1.0
Insulator plate thickness (mm)	0.63
Module height (mm)	3.9
Area to length ratio	1.27
No. of couples	127
Maximum operating hot side temperature (°C)	150
Thermal conductivity (W/m K)	1.647

The thermal and structural configurations of both models followed earlier experimental roof ventilation research conducted by Chantawong, Khedari, Waewsak, and colleagues; however, they were extended in this study to integrate thermoelectric energy-harvesting capabilities [18,23].

3.1.3 Instrumentation and data acquisition

The experiment was conducted on November 2, 2025, under natural climatic conditions. Performance measurements focused on environmental conditions, indoor thermal response, roof heat transfer, airflow characteristics, and thermoelectric output. Solar irradiance was measured using an MS-402 EKO pyranometer (0–1000 W/m² range). Air and surface temperatures were monitored using Type-K thermocouples with an accuracy of ±0.5°C, installed at the following locations: indoor air, ceiling surface, roof outer surface, roof inner layer, and within the RSCCT chimney channel. Wind speed was recorded both inside and outside the test houses using a TSI Model 8380 anemometer (0–50 m/s range; ±5% error). Roof heat flux was measured using an EKO MF-140 heat-flow meter (–20 to 120°C; ±5% error), and the thermoelectric voltage output was logged concurrently with the thermal measurements. All instruments were connected to a Hioki 8422-52 multichannel data logger with a recording accuracy of ±0.8%, sampling at 5-min intervals between 08:00 and 18:00. The measurement point locations for both the SCR and RSCCT models are illustrated

in Figure 3.2(b), which shows the positions of the thermocouples, heat flux sensors, anemometers, and thermoelectric connections.

3.1.4 The Concrete-Based Roof Solar Chimney with Thermoelectric Generator modules and Photovoltaic (PV)-assisted ventilation (CSRCT)

In this series, ten TE modules (model MT2-1, 6-127; 40 mm × 40 mm) were installed along the Concrete-Based Roof Solar Chimney with Thermoelectric Generator modules (CSRCT) around the center along the RSCCT channel. To enhance TE modules cooling and increase ventilation, a small 10-W polycrystalline photovoltaic module (25 × 36 cm², Voc = 21.6 V, Isc = 0.59 A) directly powering two DC axial fans (SAAGUCHI, Model GH8025M128; 12 V, 0.20 A; 80 × 80 mm²) positioned at the solar-chimney air inlet (ceiling level). Two openings of approximately 0.02 m² surface area were provided at outlet (ridge level). This arrangement pushed more air through the chimney channel, pulled heat out of the attic faster, and cooled the cold side of the thermoelectric modules by forced convection. A photograph of the CSRCT and SCR experimental models is presented in Figure 3.3. The two model houses were tested within the Bang Yai District, Nonthaburi Province, the experiment was conducted on April 4, 2026, under natural climatic conditions.



Figure 3-3 Schematic view of the south-facing concrete-based roof solar chimney integrated with thermoelectric modules (CSRCT) and a photovoltaic (PV)-assisted ventilation system, compared with a conventional concrete roof (top), dimensions of the experimental houses and locations of the measurement positions (bottom).

3.2 The roof solar concrete chimney integrated with a thermoelectric module

This series concerned simple configurations of roofs. For Home 1 (SFR), a conventional roof configuration was used whereas for Home 2 (FSRCT), the roof was modified to include a solar chimney with a two-layer structure. The upper layer was composed of blue pearl-colored double-corrugated fiber-cement tiles designed to enhance ventilation, while the inner layer comprised flat fiber-cement tiles with a thickness of approximately 8 mm. One TE module (model MT2-1, 6-127; 40 mm × 40 mm) with a rectangular fin heat sink was installed in the middle of the chimney channel. The gap between the upper and lower roof layers was approximately 0.01 m, thereby creating a ventilation pathway. Openings with an area of approximately 0.02 m^2 were provided at both the lower (indoor side) and upper (outdoor side) ends of the channel to promote buoyancy-driven airflow. Figure 3.4 shows a photograph of the fiber-cement solar-roof chimney combined with a thermoelectric module. Figure 3.5 presents the positions of measuring instruments inside the test house with a simple fibre-cement roof: SFR (Home 1) and a fibre-cement Solar Roof Chimney combined with a thermoelectric module (Home2). The two small experimental houses, built similar to the previous ones, were in Krabang District, Bangkok 10520, Thailand. And tested on June 27, 2025.

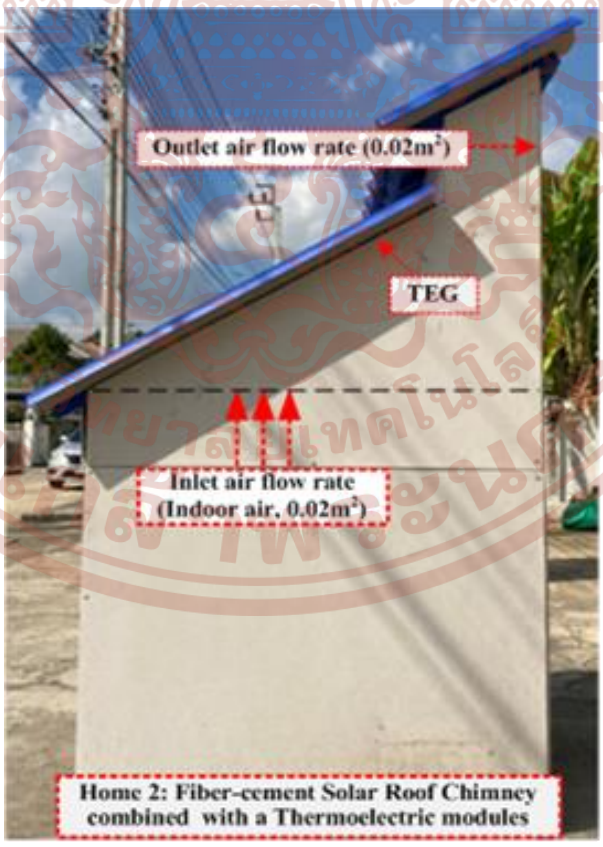


Figure 3-4 Fiber-cement solar-roof chimney combined with a thermoelectric module.

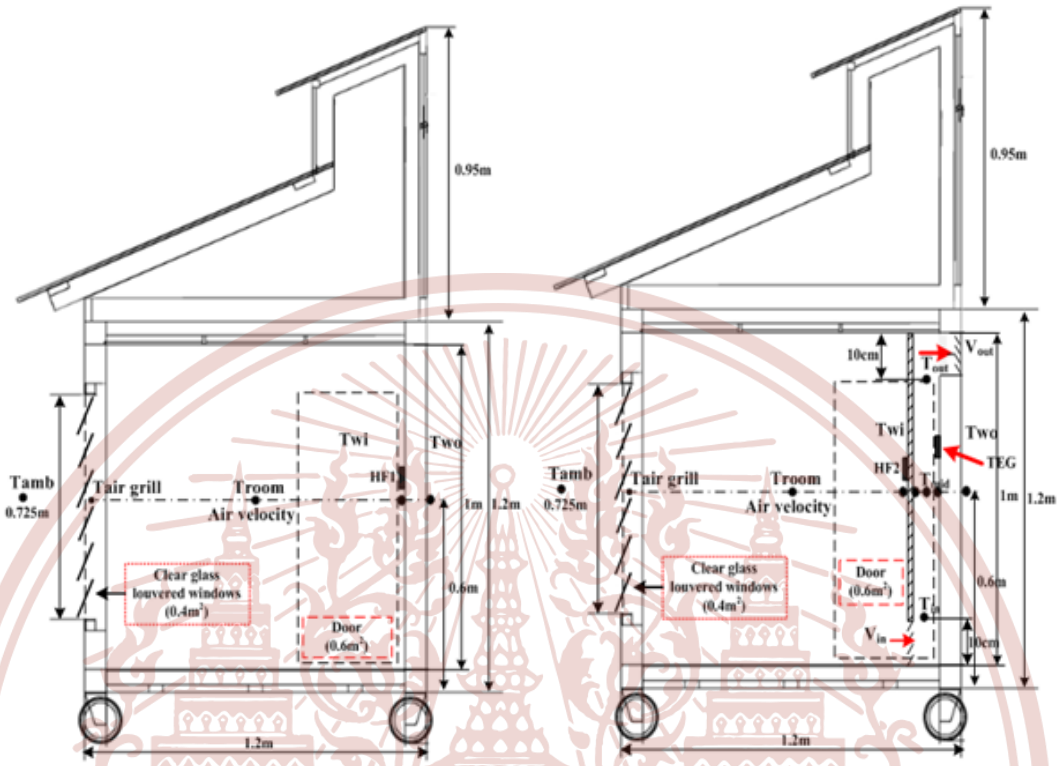


Figure 3-5 Installation of measuring instruments inside the test house with a simple fibre-cement roof: SFR (Home 1) and a fibre-cement Solar Roof Chimney combined with a thermoelectric module (Home2)

The voltage of the thermoelectric module was monitored using 20 AWG UL1007 wiring (rated at 80°C and 300 V), connected to a 1 Ω matched load resistance (Figure 3.2(a)), and the power output was calculated using Ohm's law. Data monitoring and analysis followed the same methodology in the previous configurations. All instruments were logged at five-minute intervals between 8:00 AM and 5:00 PM using a Hioki 8422-52 data logger, which has a recording accuracy of ±0.8%.

3.3 The lightweight solar wall chimney with a thermoelectric generation module

This part evaluated the thermal performance of a simple design of lightweight solar wall chimney with a thermoelectric generation module (LSWCT) designated Home 2) in comparison with a simple cement board wall (SCW; referred to as Home 1). Both systems were tested in two identical model houses, each with a volume of 2.016 m³ (Figures 3-6 and 3-7).

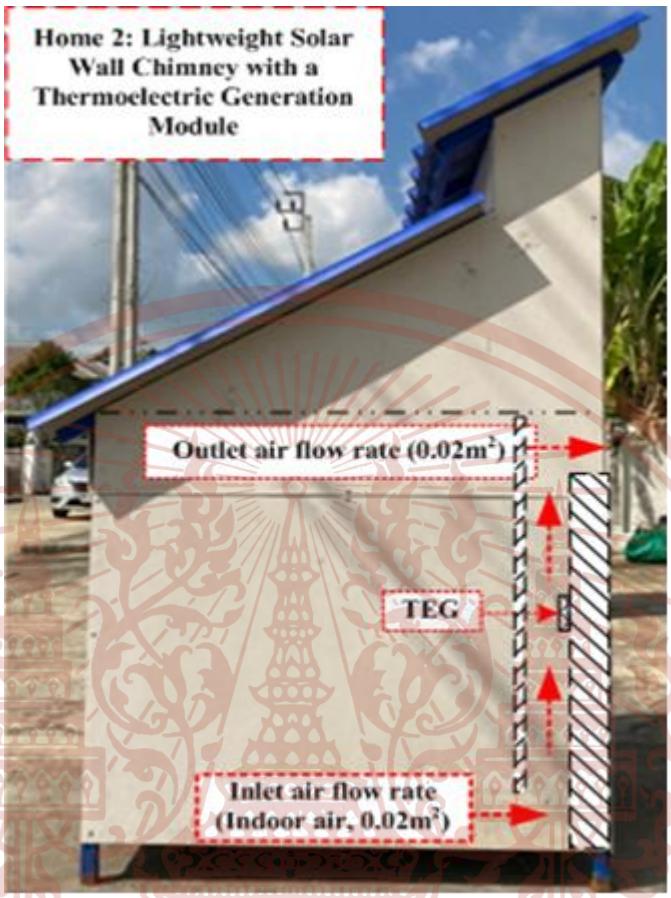


Figure 3-6 Lightweight Solar Wall Chimney with a Thermoelectric Generation Module.

The SCW has a single-layer wall structure, whereas the LSWCT integrates thermoelectric module for supplementary power generation. Experimental assessments were conducted under typical hot and humid weather conditions prevalent in Thailand. The study focused exclusively on the south-facing wall, which has an effective solar radiation area of approximately 1.44 m². The LSWCT groove wall was designed with two plaster layers, each approximately 8 mm thick, separated by a 0.01 m air gap, which facilitated natural ventilation. An MT2-1 thermoelectric module (6-127, 40 × 40 mm) with a rectangular fin heat sink was installed at the center of the chimney wall. The chimney also included a 0.02 m² opening, with the lower inlet connected to the interior of the house and the upper outlet venting outside, thereby enabling buoyancy-driven airflow. Measurements were taken on July 25, 2025. The parameters recorded during the evaluation included ambient temperature, solar radiation intensity, internal temperatures of both houses, temperature gradients within the LSWCT chimney, wind speeds measured both inside and outside the model houses, and the heat flux across the south-facing walls. Data monitoring and analysis followed the same methodology in the previous configuration.

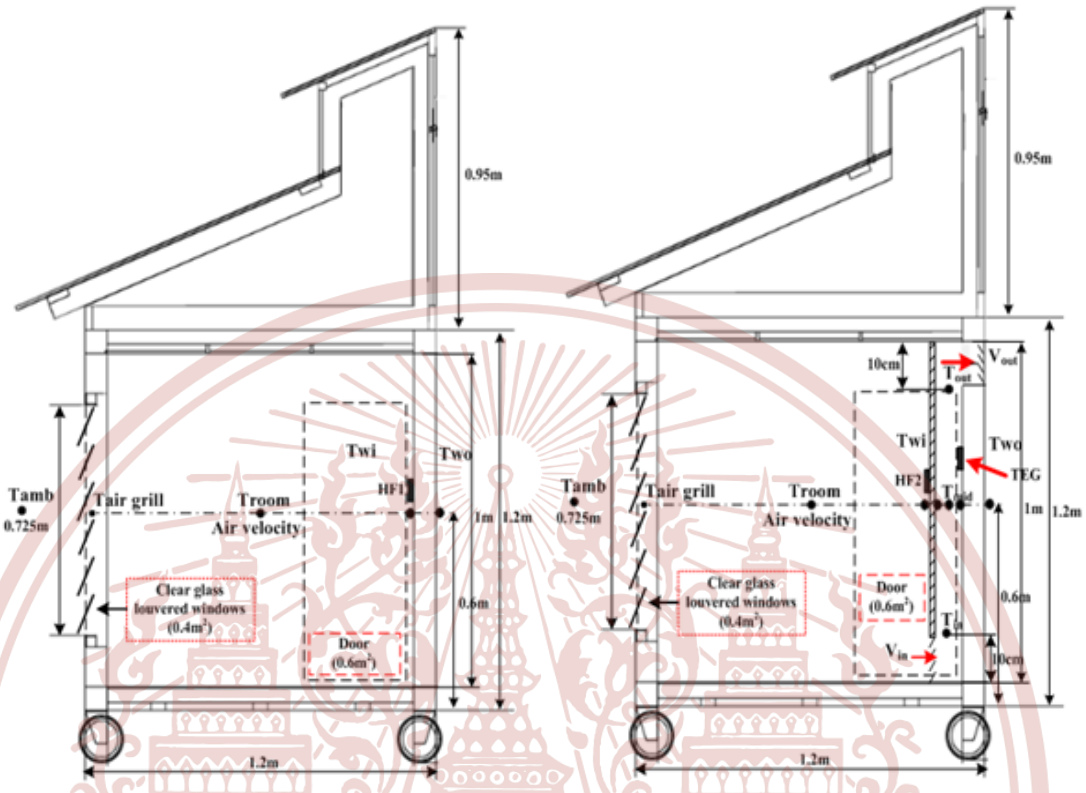


Figure 3-7 Shows the installation of measurement instruments inside a test house with a simple cement board wall (SCW; Home 1) and a lightweight solar wall chimney with a thermoelectric generation module (LSW;T: Home 2)

The two small experimental houses were located in Krabang District, Bangkok 10520, Thailand.

3.4 The Measuring Devices

To facilitate understanding, the first model house served as the reference wall and roof configuration while the second house incorporated the concrete-based roof and wall solar chimney configurations integrated with thermoelectric module. The various measured parameters included ambient temperature (Tamb), indoor air temperature (Tindo), heat flux (HF), and global solar irradiance (It) roof-surface temperature (Troof), attic or cavity temperature (Tattaic), ceiling temperature (Tcelling), air-grill temperature (Tair grill) and electrical voltage.

The intensity of solar radiation was measured using the MS 402 EKO pyranometer (Accuracy 0-1000 W/m^2) shown in figure 3-8



Figure 3-8 MS 402 EKO pyranometer

The different temperatures of both houses were measured using Type K thermocouples (range: 0-1250 ºC, accuracy ± 0.5ºC). The wind speed inside and outside the house was measured using the TSI Model 8380, range: 0 - 50 m/s, Error ± 5%shown in figure 3-9.



Figure 3-9 Hot wire anemometer

The thermocouples and electric wires were connected to a datalogger “HIOKI” model LR8400-20 (±0.2s/day @23°C) shown in figure 3-10. Data were recorded using a data logger (Hioki, Model: 8422-52, accuracy ± 0.8%) every 5 minutes from 7:00 AM to 6:00 PM.



Figure 3-10 Datalogger “HIOKI” model LR8400-20 (±0.2s/day @23°C)

EKO Heat flow meter shown in figure 3-11 Model MF-180, range: -30ºC to 120ºC, Error ± 5% was used to measure heat transmitted through internal surface of ceiling.

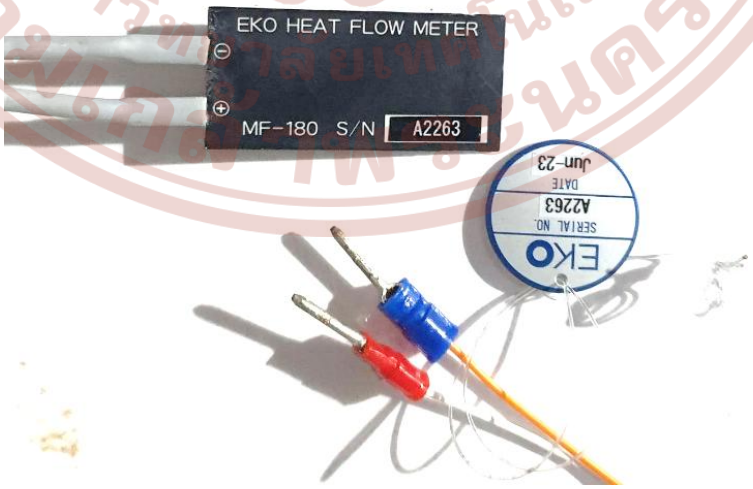


Figure 3-11 Heat flux (EKO)

Two model houses of identical size were constructed and tested in Bangkok to evaluate and compare the thermal protection performance of the wall systems. The study focused exclusively on the south-facing wall, which has an effective solar radiation area of approximately 1.44 m², under typical weather conditions. Home 1 was fitted with a single-layer cement board wall (SCW), whereas Home 2 incorporated a lightweight solar-wall chimney with a thermoelectric generation module (LSWCT).

The LSWCT groove wall was designed with two plaster layers, each approximately 8 mm thick, separated by a 0.01 m air gap, which facilitated natural ventilation. An MT2-1 thermoelectric module (6-127, 40 × 40 mm) with a rectangular fin heat sink was installed at the center of the chimney wall. The chimney also included a 0.02 m² opening, with the lower inlet connected to the interior of the house and the upper outlet venting outside, thereby enabling buoyancy-driven airflow. Both model houses had an internal volume of 2.016 m³. The roofs were inclined at 30°, with a surface area of 1.92 m², and were constructed with 6 mm fiber cement tiles as the outer layer and 6 mm gypsum board ceilings for thermal insulation. The walls were plaster-finished, painted in the same gray cream color, and 8 mm thick. Each house was fitted with a 0.6 m² hard plastic door (0.075 m thick) on the north wall, incorporating a 0.4 m² louvered section for ventilation. The materials used were consistent with previous reference standards.

The experiment was conducted under Thailand's hot and humid climatic conditions, following earlier studies by Chantawong. Measurements were performed on July 25, 2025, with the air conditioning turned off to allow natural heat transfer processes to dominate. The environmental temperature, solar radiation intensity, and internal temperatures of both model houses were recorded, along with the temperatures within the LSWCT chimney. Solar radiation was measured using an MS-402 EKO pyranometer (accuracy: 0–1000 W/m²). Temperatures were monitored using Type K thermocouples (range: 0–1250 °C, accuracy ±0.5 °C). The wind speeds inside and outside the houses were measured using a TSI Model 8380 anemometer (range: 0–50 m/s, error ±5%). The heat flux through the south-facing walls was captured using an EKO heat flow meter, MF-140 (range: –20 to 120 °C, error ±5%).

For the thermoelectric system, the voltage and current generated were measured using 20 AWG UL1007 wires (80 °C, 300 V) connected to a 1 Ω matched load resistor (Figure 3.1(b)), and the electrical power was calculated using Ohm's law. Data were acquired using a Hioki Data Logger (Model 8422-52, accuracy ±0.8%), recording measurements every 5 min between 08:00 AM and 05:00 PM. This setup ensured a rigorous and direct comparison of the thermal and electrical performances of the SCW and LSWCT systems under identical environmental conditions

CHAPTER 4
EXPERIMENTAL RESULTS

Field experiments of the various concrete-based solar chimneys presented in the previous chapter were conducted on different days during several months. The experimental campaign generated a comprehensive dataset covering the thermal, ventilation, and thermoelectric performance of the two model houses. The results are presented for the tested days and the important findings and reported and analyzed

4.1 The roof solar concrete chimney with thermoelectric modules (RSCCT).

The results enabled a detailed comparison between the behavior of a conventional fiber-cement roof (SCR) and a modified roof incorporating a solar concrete chimney with thermoelectric generation (RSCCT). The following discussion examines the temporal evolution of the environmental conditions, indoor thermal response, roof heat flux, airflow characteristics, and thermoelectric performance.4.1.1 Environmental conditions and boundary climate behavior

4.1.1 Indoor Temperature heat flux and ambient conditions

Figure 4.1 illustrates the temporal variations of ambient temperature (Tamb), indoor air temperature in both model houses, and global solar irradiance (It). Solar radiation increased rapidly after sunrise, exceeded 1000 W/m² near midday, and reached a maximum of approximately 1298 W/m² at 13:50. This pattern is characteristic of tropical clear-sky conditions and produces strong radiative incident on the roof surfaces during the late morning and early afternoon. The ambient temperature followed a similar upward trend, rising from approximately 27.5 °C in the morning to nearly 36.5 °C under the peak conditions, coinciding with the period of maximum solar intensity.

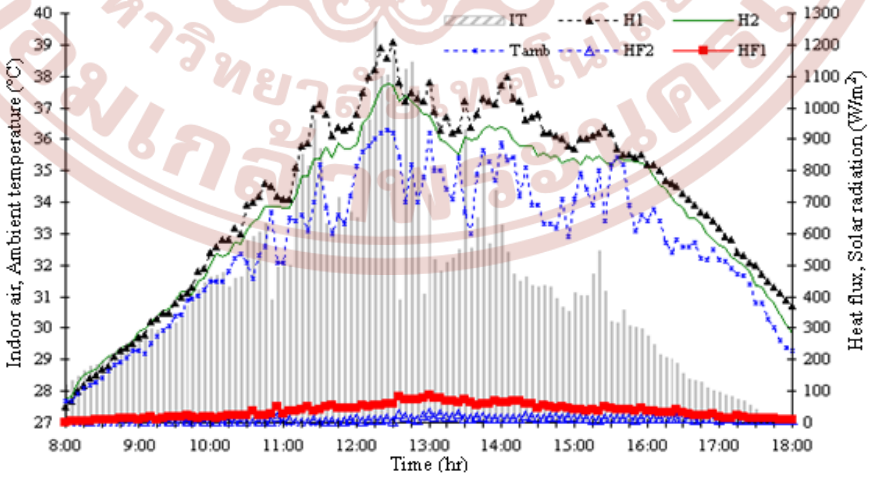


Figure 4-1 Figure 4.1 Changes in indoor temperature, ambient temperature, and solar radiation intensity (2 November 2025)

The indoor temperature showed that both houses warmed progressively as the external conditions intensified; however, their thermal responses were not identical. The house with the conventional SCR roof exhibited a sharper rise and a higher afternoon peak, indicating a stronger heat transfer and retention of solar heat within the interior space. In contrast, the house equipped with the RSCCT roof maintained lower and more moderate indoor temperatures over the same period, with a noticeably flatter temperature profile during peak-radiation hours. The difference in indoor temperature between the two homes ranged from approximately 0.2 °C in the early morning, when solar effects were minimal, to nearly 2.8 °C during the afternoon peak, when both solar radiation and ambient temperature were at their maximum. These observations provide an initial indication that the RSCCT roof attenuates and delays the indoor temperature increase under daytime heating, an effect that is examined in greater detail through the heat-flux and ventilation analyses presented in the subsequent sections.

4.1.2 Temperatures comparison between SCR and RSCCT roof configurations

Figures 4.2 and 4.3 show the hourly variations in the temperatures measured at different locations within the roof–ceiling–attic assembly for the two model houses. The monitored variables included the roof surface temperature (Troof), attic or cavity temperature (Tattaic), ceiling temperature (Tcelling), air-grill temperature (Tair grill), and ambient temperature (Tamb), allowing the heat-transfer pathway through each roof configuration to be examined.

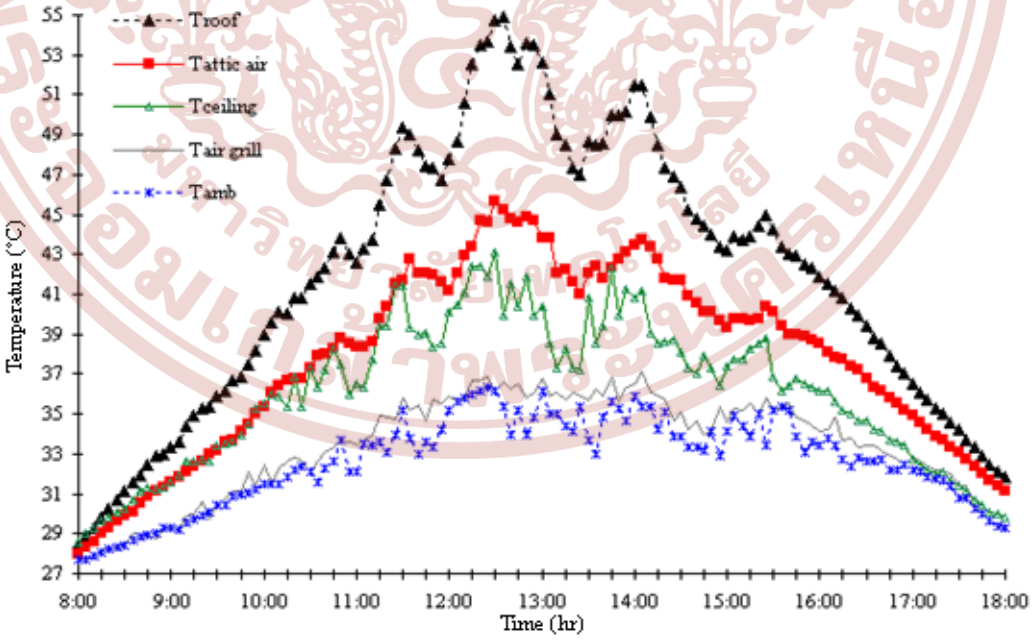


Figure 4-2 The results of temperature changes inside the installed test house with SCR (Home 1) (November 2, 2025).

In the house with the conventional SCR roof (see Figure 4.2), the temperatures at the roof surface, attic space, and ceiling layer increased markedly in the late morning and early afternoon, closely following the increase in solar radiation. The elevated values of T_{attaic} and $T_{celling}$ indicate that the heat absorbed at the outer roof surface is transmitted downward and retained within the attic cavity and ceiling board. This behavior reflects a predominantly conductive heat transfer process with limited convective removal, resulting in progressive heat accumulation above the occupied zone and contributing to indoor warming later in the day. In contrast, the RSCCT roof (see Figure 4.3) exhibited a different thermal pattern. Although the outer roof surface was exposed to the same solar incident radiation, the temperature within the chimney/ventilation channel increased significantly above the ceiling temperature, whereas the ceiling and air-grill temperatures remained comparatively lower than those in the SCR case. The higher air-channel temperature relative to the ceiling indicates the formation of buoyancy-driven upward airflow, which transports heated air out of the roof cavity rather than allowing it to be conducted toward the interior. Consequently, the RSCCT configuration reduced the thermal storage at the ceiling plane and limited the downward heat transfer into the room.

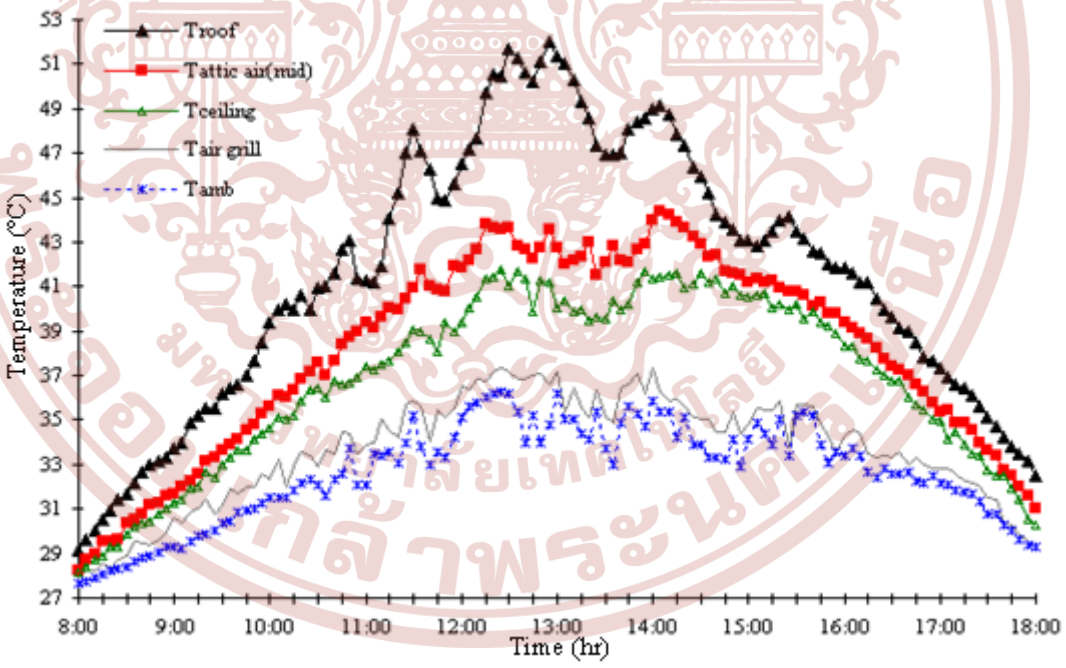


Figure 4-3 The results of temperature changes inside the test house with the RSCCT (Home2) on November 2, 2025.

Taken together, Figures 4.2 and 4.3 demonstrate that the improvement in thermal performance provided by the RSCCT roof does not arise solely from reduced heat magnitude, but from a fundamental change in the heat-transfer pathway. In the SCR roof, heat is absorbed and stored within the attic ceiling layers, whereas in the RSCCT roof, it is redirected and dissipated through the ventilated chimney channel. This mechanism explains the lower heat flux values and moderated indoor-temperature response discussed in subsequent sections.

4.1.3 Temperature stratification in the RSCCT configuration

Figure 4.4 presents the temporal variation of the air temperature at the chimney inlet (T_{tin}), mid-channel (T_{mid}), chimney outlet (T_{out}), and ambient temperature (T_{amb}) for the RSCCT house (Home 2). The three channel temperatures observed thermal stratification ($T_{tin} < T_{mid} < T_{out}$) across much of the daytime higher and remained higher than Tamb during the main solar-heating period. This indicates that the air within the RSCCT is solar-heated above ambient and it is derived by the upward buoyancy-induced airflow.

The air entering the chimney at Ttin warms further along the channel, as shown by the increase in Tmid, and reaches its highest temperature at the outlet (Tout). This progression demonstrates that the chimney acts as a thermal pathway that absorbs heat from the roof surfaces and transports it upward rather than allowing it to be conducted toward the ceiling. The higher outlet temperature relative to both Tmid and Tamb confirms that the heated air is exhausted to the exterior, thereby providing continuous removal of accumulated heat from the roof–ceiling region. This temperature stratification, therefore, explains the reduced heat flux and moderated indoor temperatures reported in subsequent sections: instead of being stored within the attic and ceiling layers, a significant portion of the absorbed solar energy is redirected and dissipated through buoyancy-driven ventilation in the RSCCT channel

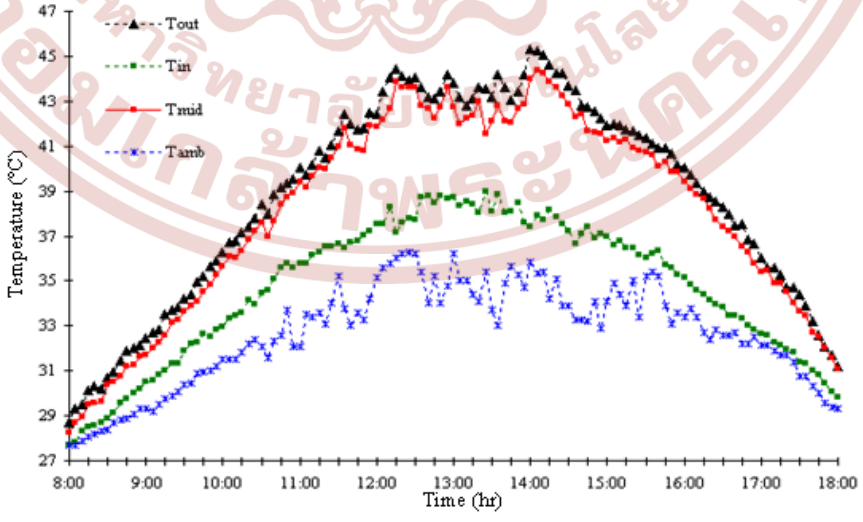


Figure 4-4 Results of temperature changes inside the RSCCT (Home 2) (November 2, 2025).

4.1.4 Thermoelectric performance

Figure 4.5 shows the variations in ambient temperature (Tamb), the temperature difference across the thermoelectric module, and the corresponding electrical power output for the RSCCT house (Home 2). The ambient temperature follows the daytime profile described in Figure 4.1, rising from the high-20s °C in the morning to the mid-30s °C in the afternoon. In contrast, the thermoelectric modules temperature difference remained close to zero in the early morning and then increased sharply as solar radiation intensified, and the roof surface and chimney-channel temperatures increased. This behavior indicates that the thermoelectric modules begin to operate effectively only after a sufficient temperature gradient is established between their hot and cold sides.

As the TE module temperature difference increases, the TE power output increases in parallel, reflecting the Seebeck effect that governs TE modules operation. During the main solar-heating period, the power generated by the TEGs ranges from approximately 0.12 to 1.8 mW, with the peak output occurring around the time of maximum thermoelectric modules temperature difference. This confirms that the RSCCT system successfully converts part of the roof-surface heat into electrical energy, even though the available temperature differences are relatively modest. When the solar intensity and chimney temperatures decline in the late afternoon, the thermoelectric modules temperature differences decreases, and the electrical output falls accordingly, demonstrating the strong coupling between thermal conditions and thermoelectric performance.

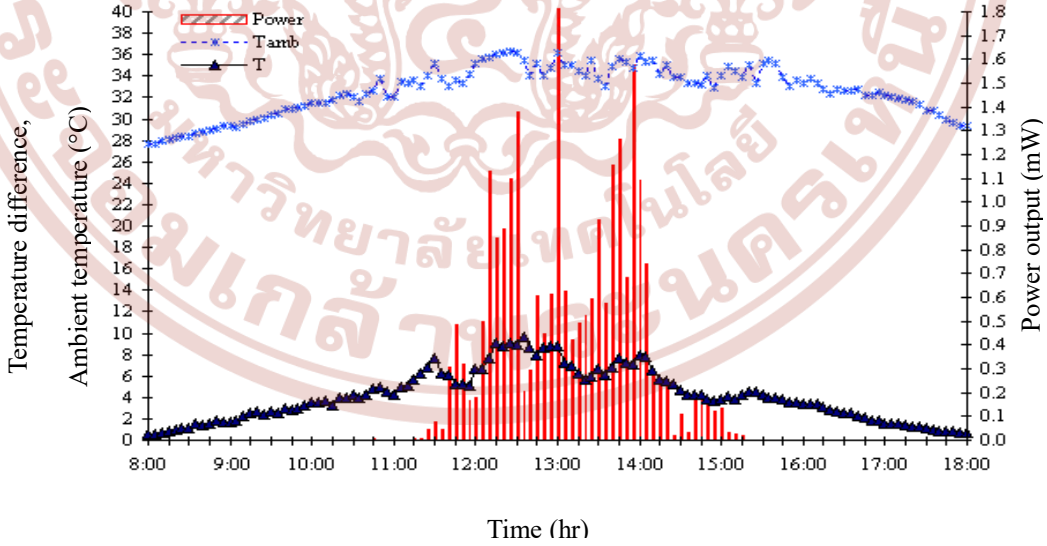


Figure 4-5 Results of the temperature change of the ambient, the temperature difference of the thermoelectric, and the power output (Home 2), (2 November 2025)

Although the generated power is small, it highlights the feasibility of low-grade heat harvesting in a building-integrated configuration. In practical terms, the measured output is sufficient for ultra-low-power applications, such as wireless temperature or airflow sensors, status indicators, and other Internet of Things devices embedded in the roof system. Importantly, this energy-harvesting function is achieved without compromising the primary role of the RSCCT in reducing roof heat gain and enhancing natural ventilation. Instead, the thermoelectric modules utilize the same temperature gradient that drives buoyancy in the chimney channel, providing a useful co-benefit that complements the passive cooling performance of the roof. ance, ventilation behavior, and thermoelectric output of the two model houses.

4.2 The Concrete-Based Roof Solar Chimney with Thermoelectric Generator modules and Photovoltaic (PV)-assisted ventilation (CSRCT)

4.2.1 Indoor Temperature, heat flux and ambient conditions

Figure 4.6 illustrates the transient responses of ambient temperature (Tamb), indoor air temperature in the two experimental houses (Home 1: SCR and Home 2: CSRCT), heat flux (HF1 and HF2), and global solar irradiance (It) during the monitoring period. Global solar irradiance increased sharply after sunrise and exceeded 1,000 W m^{-2} near midday, reaching a peak value of approximately 930 W m^{-2} at 12:35 h. Clear-sky days in the tropics regularly show this kind of curve, and the high irradiance drove large radiative heat gains at the roof surfaces. Ambient temperature climbed from about 37.7 °C to nearly 38 °C over the same hours.

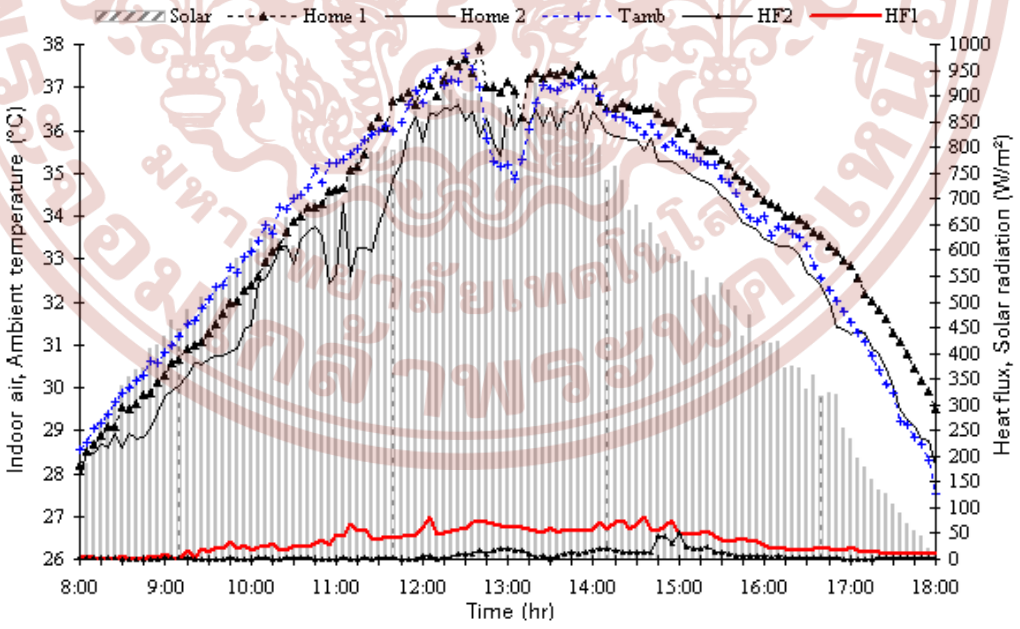


Figure 4-6 Changes in indoor temperature, ambient temperature, Heat flux and solar radiation intensity (April 4, 2026)

Similar to the previous section, figure 4.6 shows that both houses got warmer as the day went on, but not at the same rate. The SCR house heated up faster and peaked higher in the afternoon, a sign that more solar heat was getting through and staying inside. By contrast, the house equipped with the CSRCT roof maintained lower and more moderate indoor temperatures over the same period, with a noticeably flatter temperature profile during peak-radiation hours. As read from figure 4.6, the difference in indoor temperature between the two model houses ranges from approximately 0.2 °C in the early morning, when solar effects are minimal, to nearly 3.2°C during the afternoon peak, when both solar radiation and ambient temperature are at their maximum. These observations indicate that the CSRCT roof can also attenuate and delay the indoor temperature rise under daytime heating. The net benefit of this is examined in greater detail through the heat-flux and ventilation analyses. It was observed a 78.5% drop in average roof heat flux compared to the CSR that's extremely interesting; and contributed to lower indoor air temperature, with the CSRCT house remaining 0.2–3.2°C cooler than the SCR house during the hottest part of the day.

4.2.2 Air velocity and PV power output

Figure 4.7 shows the indoor air velocity in both houses, together with the outdoor wind speed and airflow velocity within the CSRCT channel, and power generated by the PV panle. The CSRCT house consistently exhibited higher indoor air velocities (0.54–0.94 m/s) than the reference SCR house (0.020–0.045 m/s).

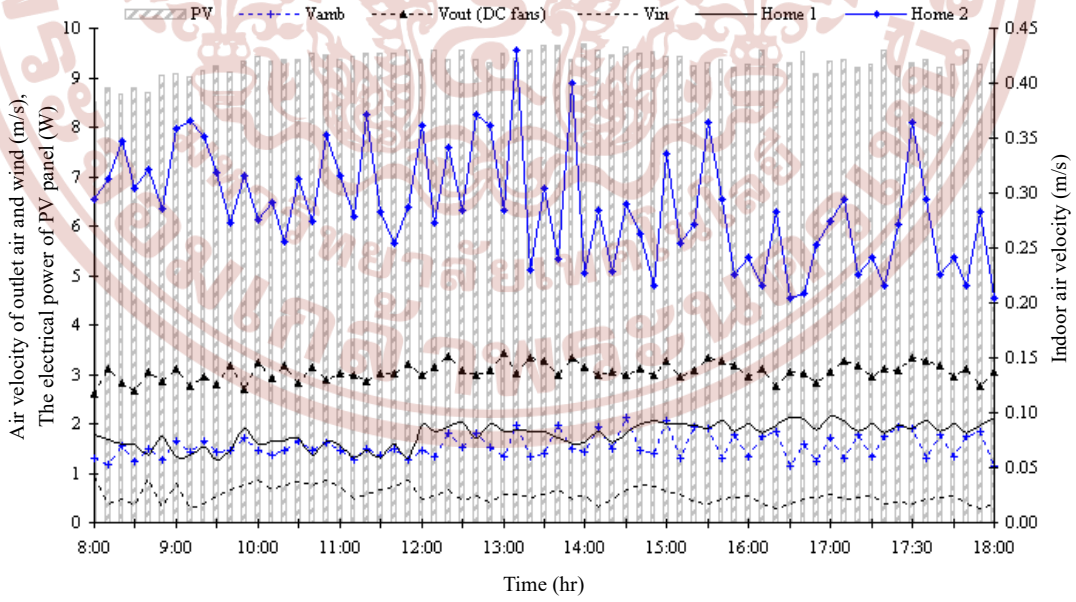


Figure 4-7 Hourly variations of indoor air velocity, outlet air of the CSRCT and wind (m/s) of the two homes and the electrical power of PV panel (April 4, 2026).

The PV panel generated an electrical output varying between 2 and 9.7 W and powered the two small DC fans speeding up or slow down with the changing solar radiation. Outlet air in the CSRCT channel hit 2.5–3.2 m/s, fast enough to pull heat out of the roof cavity effectively. In contrast, under non-fan operation, the channel airflow varied with natural ventilation, ambient conditions, and wind speed. The increased ventilation rate in the CSRCT system enhanced convective heat dissipation, which cut roof heat buildup and helped keep indoor temperatures down.

4.2.3 Temperatures comparison between the CSRCT and CSR configurations

Figures 4.8 and 4.9 plot temperatures at five positions in each house. The monitored variables are the roof-surface temperature (Troof), attic or cavity temperature (Tattaic), ceiling temperature (Tcelling), air-grill temperature (Tair grill), and ambient temperature (Tamb).

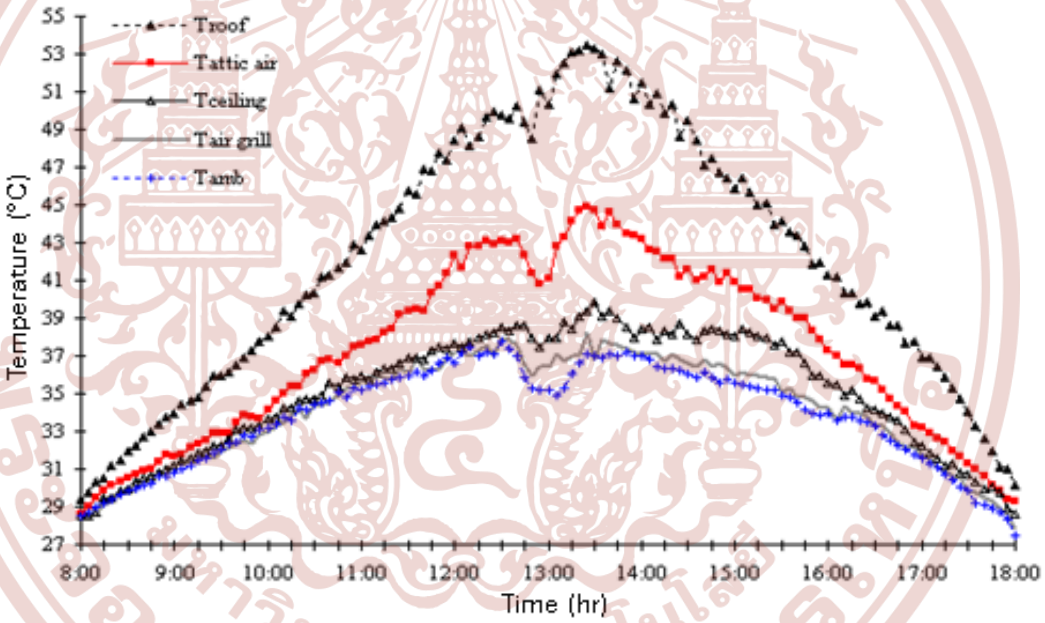


Figure 4-8 The results of temperature changes inside the installed test house with a SCR (Home 1) (April 4, 2026)

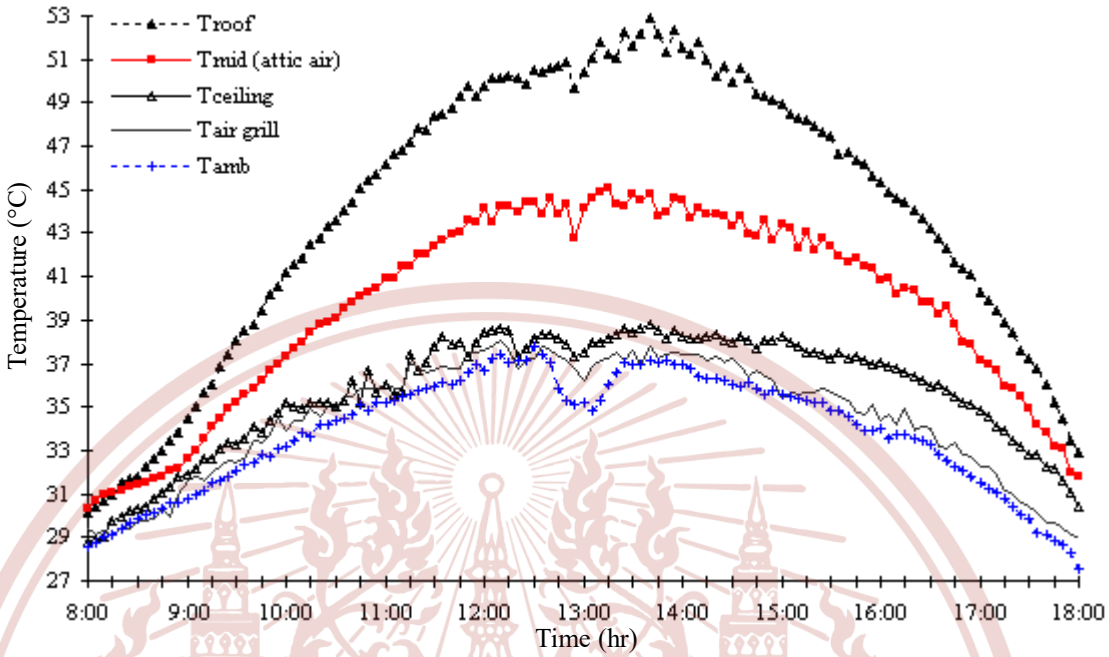


Figure 4-9 The results of temperature changes inside the installed test house with CSRCT (Home2). (April 4, 2026).

The observations discussed in the previous are valid for these configurations too. Under the SCR roof (Figure 4.8), roof-surface, attic, and ceiling temperatures all climb steeply from late morning into the early afternoon, tracking the solar radiation. The elevated values of Tattaic and Tcelling indicate that heat absorbed at the outer roof surface is transmitted downward and retained within the attic cavity and ceiling board. Convection removes very little of it, so heat keeps piling up above the living space and warms the rooms later in the day. By contrast, the CSRCT roof (Figure 4.8) exhibits a different thermal pattern. Although the outer roof surface is exposed to the same solar heat, the temperature within the chimney/ventilation channel rises significantly above the ceiling temperature, while the ceiling and air-grill temperatures remain comparatively lower than in the SCR case. Hot air rises through the channel and exits the roof instead of conducting downward. Consequently, the CSRCT configuration reduces thermal storage at the ceiling plane and limits downward heat transfer into the room.

Figures 4.8 and 4.9 demonstrate that the improvement in thermal performance provided by the CSRCT roof does not arise solely from reduced heat magnitude, but from a fundamental change in the heat-transfer pathway. In the SCR roof, heat is absorbed and stored within the attic–ceiling layers, whereas in the CSRCT roof it is redirected and dissipated through the ventilated chimney channel with ventilated much enhanced by the PV panel.

4.2.4 Temperature Stratification in the CSRCT configuration

Figure 4.10 presents the temporal variation of the air temperature at the chimney inlet (T_{tin}), mid-channel (T_{mid}), chimney outlet (T_{out}), and ambient temperature (T_{amb}) for the CSRCT house (Home 2). The discussion reported in section 4.1.3 is valid but with a different temperature behavior namely between air temperature at inlet and mid/outlet of the chimney. It can be seen that there is no significant temperature difference between the mid and channel outlet due to the highest ventilation flowrate by the DC fans that reduced thermal stratification. This is due to the forced ventilation and short chimney length.

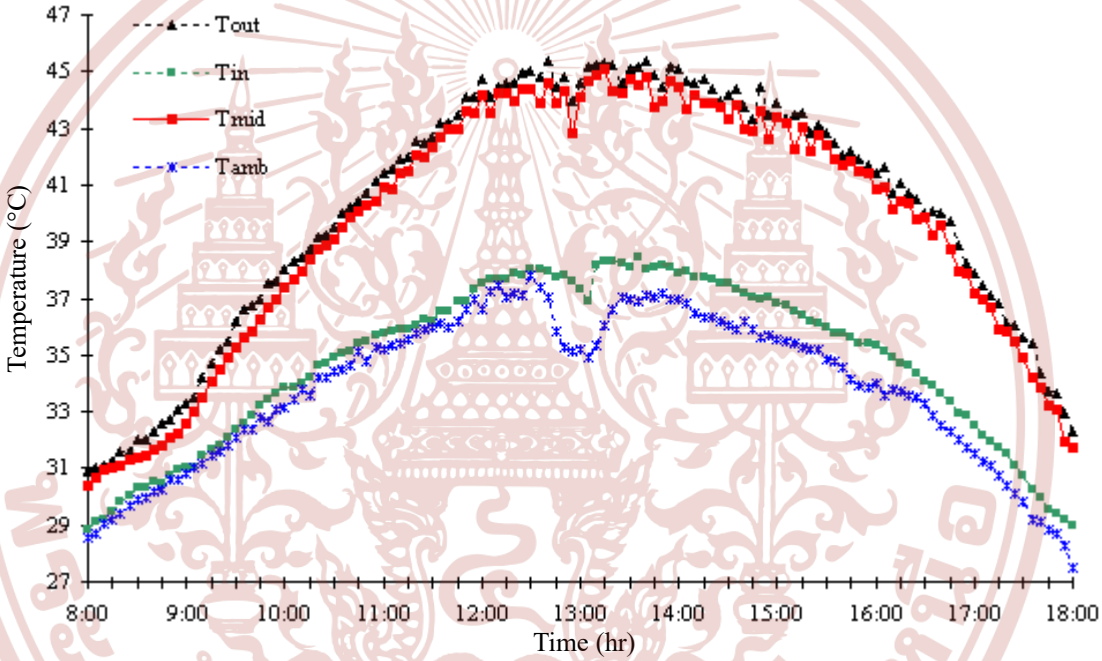


Figure 4-10 Results of temperature changes inside the CSRCT (Home 2).(April 4, 2026).

4.2.5 Thermoelectric Performance

Figure 4.11 presents the variation of ambient temperature (Tamb), the temperature difference across the thermoelectric modules, and the corresponding electrical power output for the CSRCT house (Home 2). The ambient-temperature curve follows the daytime profile described in Figure 4.6, rising from the high-20s °C in the morning to the mid-30s °C in the afternoon. In contrast, the TE modules temperature difference remained near zero early in the morning, then climbs rapidly once the sun heats the roof surface and chimney channel enough. The modules only start producing useful power after the hot side gets noticeably warmer than the cold side.

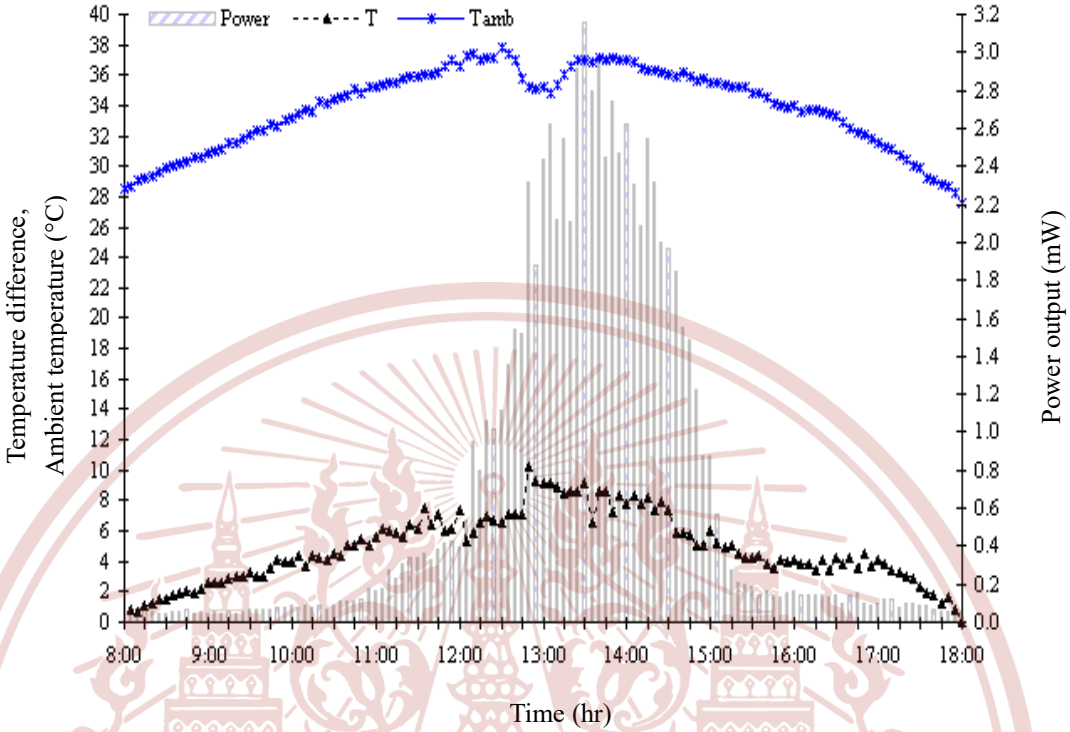


Figure 4-11 Results of the temperature change of the ambient, the temperature difference of the thermoelectric, and the power output (Home 2). (April 4, 2026).

During the main solar-heating period, the power generated by the TEGs ranges from approximately 0.04 to 3.16 mW, with peak output occurring around the time of maximum thermoelectric module, the fans increase the ventilation rate by inducing forced airflow from the indoor space to the attic and enhance heat dissipation from the thermoelectric modules through forced convective heat transfer. Thus, the overall thermal performance of the system and electrical power generation are improved. Here too, it is well confirmed that the CSRCT system successfully converts part of the roof-surface heat into electrical energy, even though the available temperature differences are relatively modest compared with conventional high-temperature thermoelectric applications. The generated power is small in absolute terms, but it shows that low-grade heat harvesting in a building-integrated setup works.

4.3 The conventional fibre-cement roof solar concrete chimney integrated with a thermoelectric module (FSRCT)

Figure 4.12 illustrates the variations in indoor temperature, ambient temperature (Tamb), and solar radiation intensity (It) during the test period of a conventional fibre-cement roof solar concrete chimney integrated with a thermoelectric module (FSRCT) compared to a simple SFR house as designed in chapter 3. The ambient temperature ranged between 26.5 and 38.5°C, whereas the solar radiation intensity varied between 0.77 and 1088 W/m², peaking around 1:50 PM. A comparison of the heat fluxes (HF1 and HF2) revealed that the model house with the FSRCT chimney roof (Home 2) experienced significantly lower heat transfer through the roof than the house with the SFR (Home 1). Specifically, the FSRCT reduced roof heat conduction by approximately 75.6% over the course of the day, highlighting the system's capacity to mitigate heat accumulation

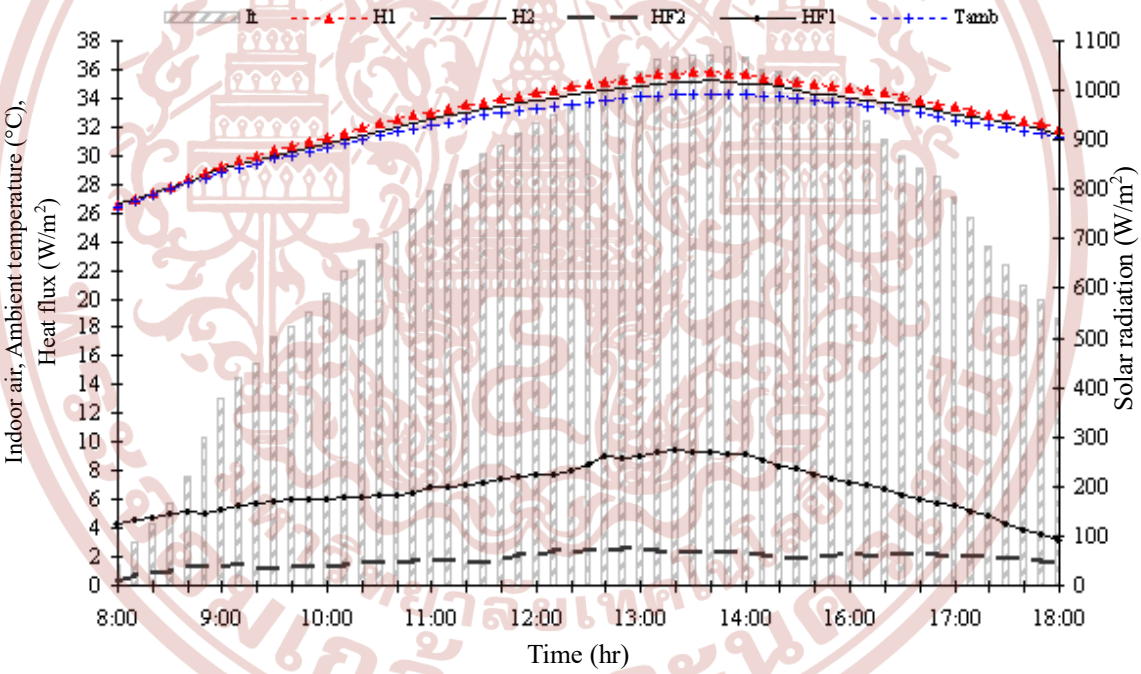


Figure 4-12 Changes in indoor temperature, ambient temperature, heat flux, and solar radiation intensity on June 27, 2025.

The temporal evolution of indoor temperatures in the two houses is shown in figures 4.12-4.14. Home 2, equipped with the FSRCT, maintained an indoor temperature approximately 0.2–1.8°C lower than that in Home 1 throughout the day. Although the roof surface temperatures were similar for both houses, the temperature inside the FSRCT chimney was consistently higher than that of the indoor and ambient air. This thermal gradient generates buoyancy-driven airflow, thereby enhancing natural ventilation.

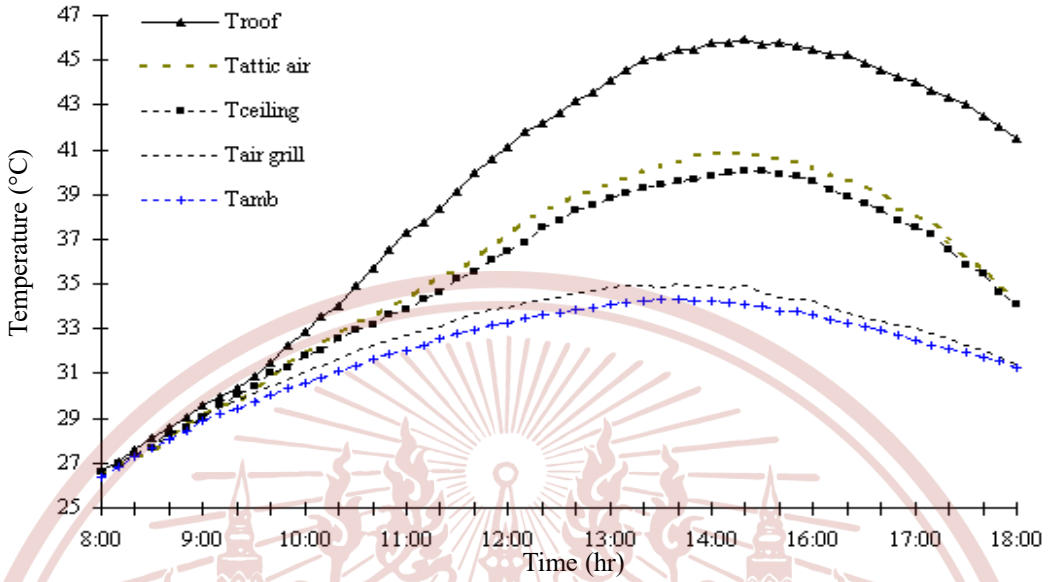


Figure 4-13 Results of temperature changes inside the test house with a simple fiber-cement roof: SFR (House 1), June 27, 2025.

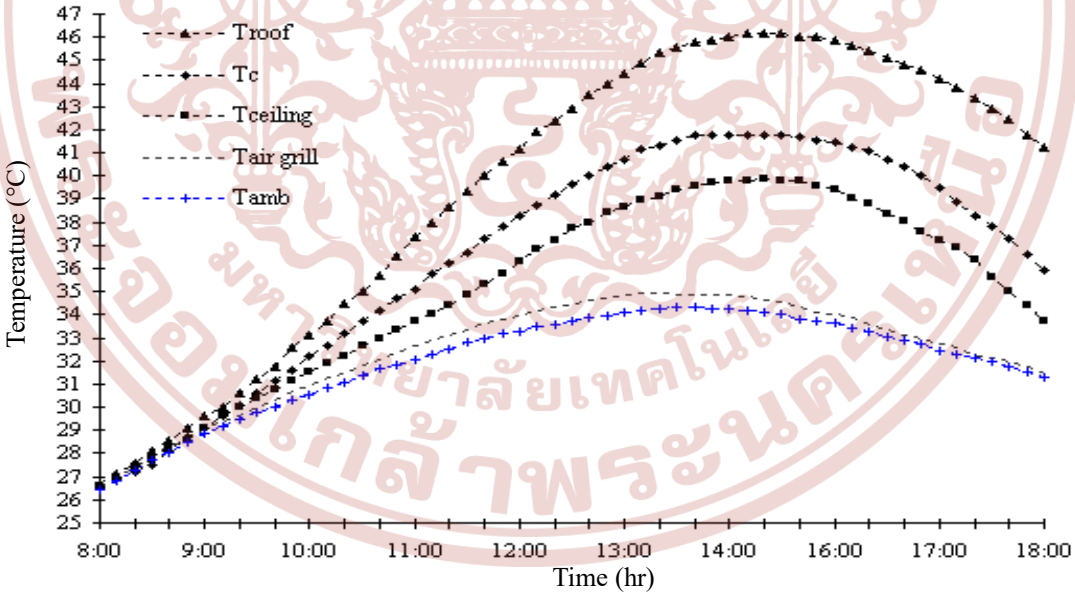


Figure 4-14 Results of temperature changes inside the installed test house with a Fibre-cement Solar Roof Chimney combined with a thermoelectric module (Home2), June 27, 2025.

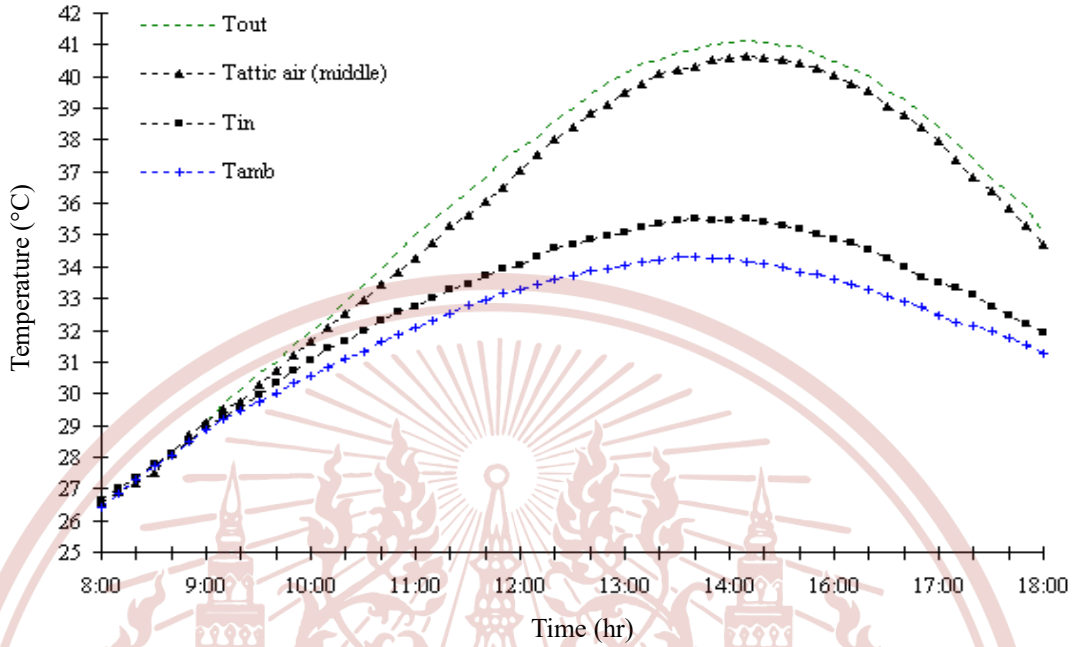


Figure 4-15 Results of temperature changes inside the fiber-cement solar roof chimney combined with a thermoelectric module (Home 2), June 27, 2025

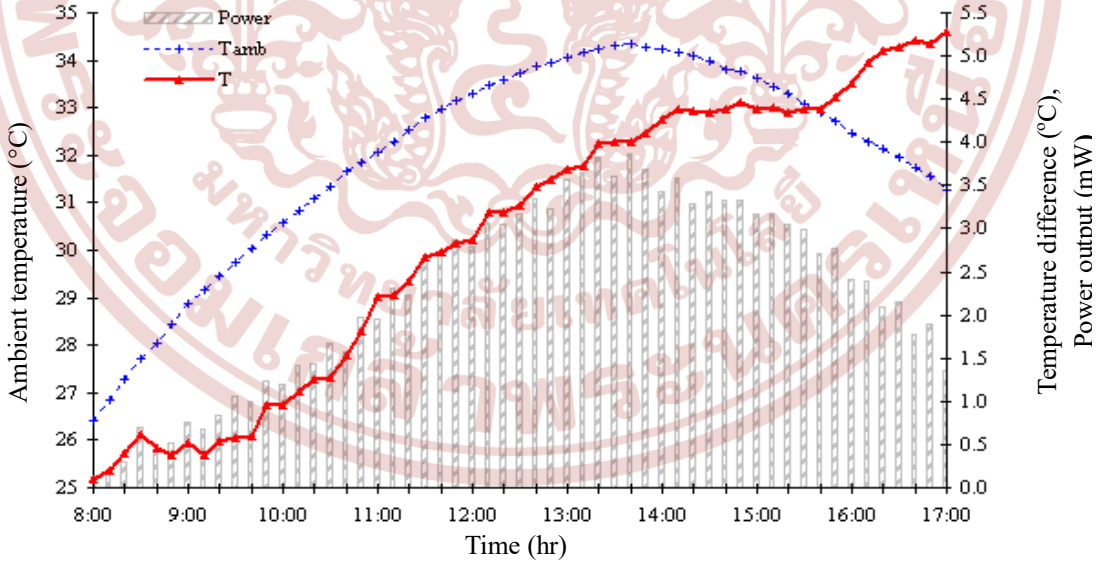


Figure 4-16 Results of temperature changes inside the fibre-cement solar roof chimney combined with a thermoelectric module (Home 2), 27 June 2025.

The electrical performance of the thermoelectric module is shown in Figure 4.16. The power generation ranged from 0.12 to 3.8 mW, depending on the temperature difference between the hot and cold sides of the module. Although modest, this output demonstrates the potential of the FSRCT system to provide supplementary power in addition to its primary function of improving indoor thermal comfort.

4.4 The conventional lightweight solar wall chimney with a thermoelectric generation module (LSWCT)

Figure 4.17 illustrates the variations in ambient temperature and solar radiation intensity throughout the test day and a comparison of the heat flux through the walls of the two model houses as discussed in chapter 3. The results showed that the solar radiation intensity gradually increased during the morning and reached a maximum of approximately 920 W/m² at 12:55 PM. The house equipped with the lightweight solar wall chimney (LSWCT) consistently exhibited lower heat flux values than the house with a simple cement board wall (SCW). On average, the LSWCT reduced the wall heat transfer by approximately 29.3%, demonstrating its superior insulating capacity.

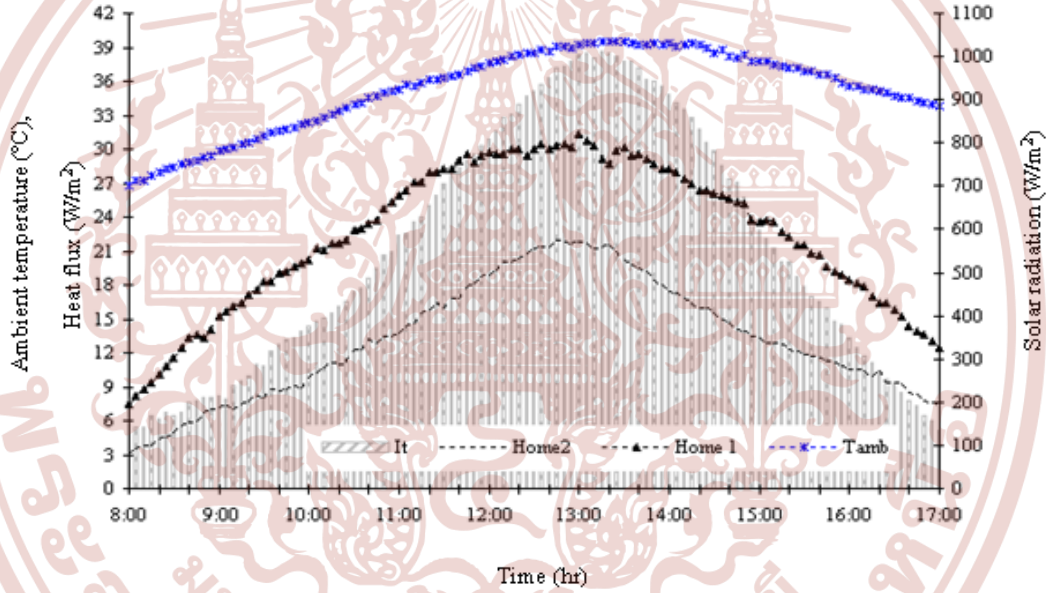


Figure 4-17 Daily variations in ambient temperature and solar radiation intensity, as well as heat flux through the walls of the SCW and LSWCT model houses, July 25, 2025.

Figures 4.17 and 4.18 present the temperature profiles inside the two houses, along with the daily variations in the outdoor ambient temperature (Tamb), which ranged from 27 to 38.8°C. The LSWCT house maintained lower indoor air temperatures than the SCW house, with reductions of approximately 0.12–2.5°C across the test period. This indicates that the LSWCT design contributed to a measurable improvement in indoor thermal comfort under hot and humid conditions. In terms of airflow performance, the LSWCT house demonstrated enhanced natural ventilation. The internal air circulation reached 0.01–0.65 m/s, substantially higher than that in the SCW house, which achieved only 0.01–0.013 m/s. The external wind speeds were measured at 1.2–2.5 m/s, whereas the LSWCT outlet maintained discharge velocities between 0.8–1.05 m/s. These results confirm that the solar

chimney wall effectively promoted buoyancy-driven airflow, reducing heat accumulation and improving ventilation within the living space. In addition to thermal benefits, the LSWCT also provided supplementary power generation. The integrated thermoelectric module produced direct current electricity ranging from 0.11 to 3.2 mW, depending on the temperature difference between its hot and cold sides. Although modest, this demonstrates the feasibility of coupling thermoelectric technology with passive cooling systems to provide added value in terms of renewable electricity generation.

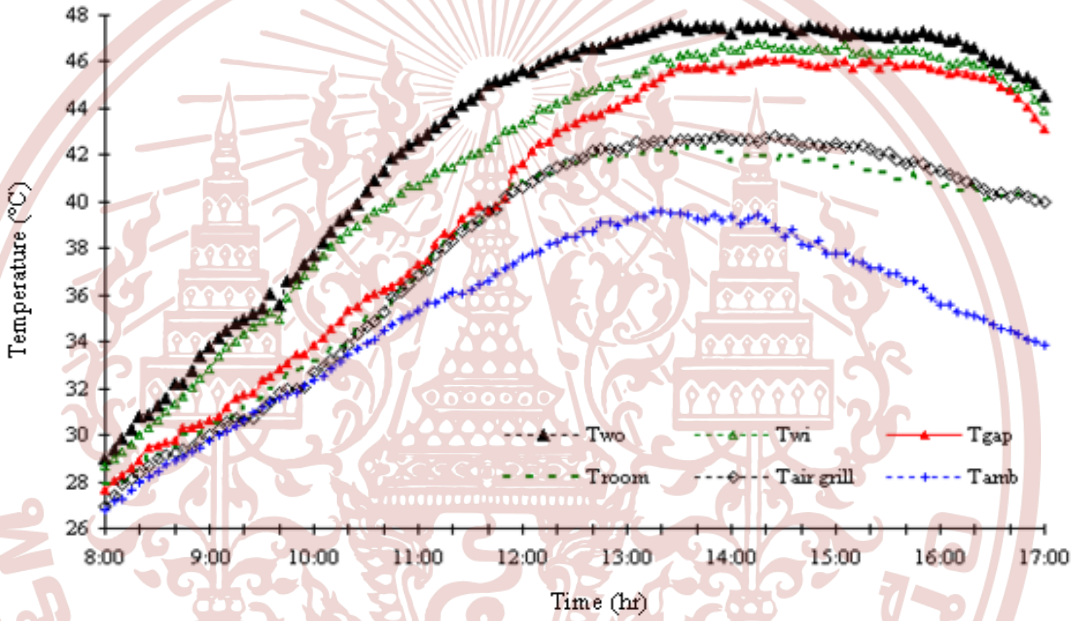


Figure 4-18 Temperature change results inside the test house equipped with a simple cement board wall (SCW; Home 2), July 25, 2025.

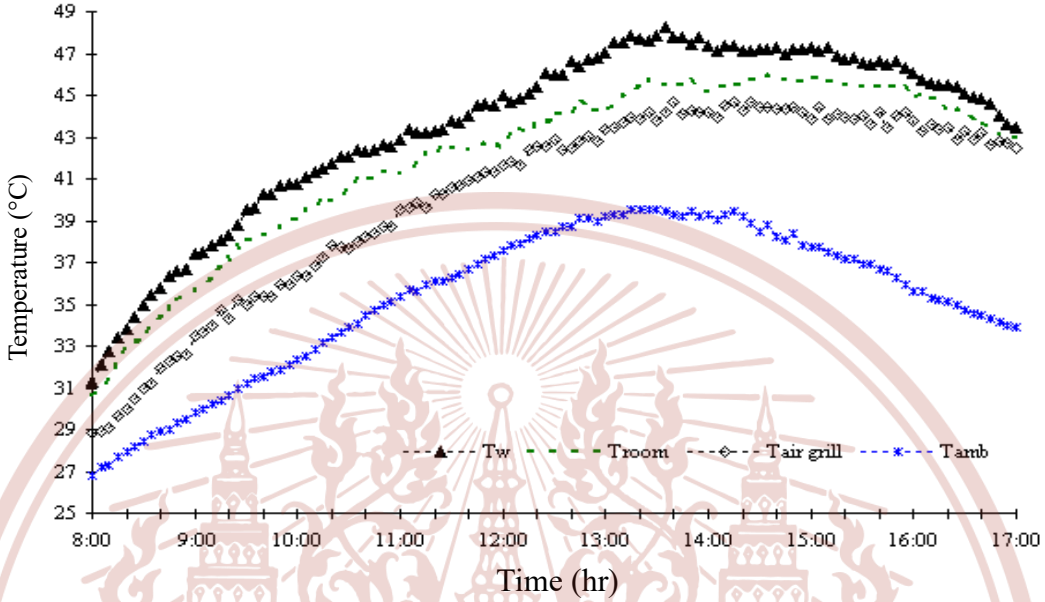


Figure 4-19 Temperature change results inside a test house equipped with a lightweight solar wall chimney with a thermoelectric generation module (LSWCT: Home 2), July 25, 2025.

Overall, this study highlights the dual functionality of the LSWCT system: (i) improved thermal insulation and indoor comfort compared with standard single-layer walls and (ii) supplementary clean energy generation. The system has a simple design, is adaptable for residential construction, and is based on locally available low-cost materials, making it a practical alternative for energy-efficient buildings in hot-humid climates.

CHAPTER 5
CONCLUSION AND RECOMMEDATION

5.1 Conclusion

Different concrete-based solar chimney configurations were designed, assembled and tested. The first is a Concrete Roof Solar Chimney made from undulating fiber-cement panels with Thermoelectric modules (CSRCT). Several cases were investigations by varying the number (one and ten) and alignment of TE modules. Also, two options were adopted for cooling the thermoelectric modules either naturally by the chimney induced ventilation or assisted using two small DC fans connected directly to a small Photovoltaic (PV) panel. The second series considered a Lightweight Solar Wall Chimney with a thermoelectric module (LSWCT). The thermal performances of these different configurations of concrete-based solar chimneys are compared to a Simple fiber-cement Roof (SFR) and a Simple Cement Wall (SCW) configuration respectively.

More precisely, the dissertation experimentally examined the thermal and ventilation performance of roof and wall concrete-based solar chimney integrated with thermoelectric power generation and compare them to a conventional fiber-cement roof and wall configurations in the hot-humid climate of Thailand. The electrical power generated by the TE modules was measured and reported. Field tests were conducted using two small houses (2.016 m3; 1.2 m x1.2 m x 1.2 m) built using white-painted fiber cement and gypsum boards for the walls. The concrete roof faced south.

The results demonstrated that all configurations considered well behaved: They significantly improve the thermal behavior of the building envelope by simultaneously reducing heat gain, enhancing buoyancy-driven ventilation, and enabling low-grade heat energy harvesting. The measurements revealed that the concrete-based solar chimney configurations altered the dominant heat transfer pathway within the roof–ceiling–attic system. In contrast to the SCR roof, which stored heat within the attic and ceiling layers, resulting in progressive conductive heat transfer toward the interior, the RSCCT redirected the absorbed solar energy into the chimney channel, where it was removed through upward airflow and exhausted to the exterior. This mechanism contributed to lower indoor air temperatures, with the RSCCT house remaining 0.2–2.8°C cooler than the reference structure during the daytime peak period. The temperature-stratification results confirmed the chimney effective buoyancy-driven ventilation and continuous heat extraction from the roof region. Accordingly, the ventilation performance improved, with internal airflow velocities increasing from 0.01–0.015 m/s in the SCR house to 0.013–0.75 m/s in the RSCCT house. These findings highlight the potential of the RSCCT system to mitigate attic heat

accumulation, reduce reliance on mechanical cooling, and enhance passive thermal comfort in tropical residential buildings.

In addition to its passive cooling function, the RSCCT enabled the TE modules to generate electricity by exploiting the temperature difference along the chimney channel. The integrated TE modules produced 0.12–1.8 mW of electrical power during peak operation, demonstrating the feasibility of building-integrated microscale energy harvesting. The Wall configuration exhibited similar performance.

These performances improved considerably when PV-assisted ventilation was considered in the roof configuration. Forced ventilation by the two small DC fans enhanced TE cooling and heat reduction. The net effect was a 78.5% drop in average roof heat flux; and contributed to lower indoor air temperatures, with the CSRCT house remaining 0.2–3.2°C cooler than the SCR house during the hottest part of the day Ventilation performance improved accordingly, with internal airflow velocities increasing from 0.020–0.045m/s in the SCR house to 0.54–0.94 m/s in the CSRCT house. It produced 0.04-3.16 mW during operation

Overall, the study confirms that concrete-based solar chimneys are practical, and energy-conserving strategy that simultaneously enhances passive cooling, promotes natural ventilation, and enables supplementary electricity generation. This approach is particularly valuable for low-rise residential buildings in tropical and subtropical regions where high solar exposure and limited attic ventilation contribute to indoor overheating and increased cooling demand. By incorporating these technologies into urban development, we can create more sustainable living environments that enhance occupant comfort while contributing to meaningful reductions in energy consumption and carbon emissions.

Finally, this thesis demonstrated that an all-solar concrete roof and lightweight solar wall configurations not only help transfer unwanted heat out of the house but also induce ventilation, which improves indoor thermal comfort and generates electrical current.

5.2 Recommendation

Future work should focus on long-term field monitoring, performance assessment across seasonal and climatic variations, and parametric design optimization, including chimney geometry, airflow channel dimensions, and thermoelectric integration layouts. Further investigation at a full-scale residential scale, as well as techno-economic and life-cycle evaluations, will support the development of RSCCT, FSRCT, and LSWCT systems as scalable and sustainable roof and wall technologies for climate-responsive housing.

REFERENCES

1. Al-Obaidi, K. M., Ismail, M., & Abdul Rahman, A. M. (2014). Passive cooling techniques through reflective and radiative roofs in tropical houses in Southeast Asia: A literature review. *Frontiers of Architectural Research, 3(3),* 283–297. https://doi.org/10.1016/j.foar.2014.06.002 [2]
2. Amornleetrakul, O., Puangsombut, W., & Hirunlabh, J. (2014). Field investigation of the small house with the ventilated roof tiles. *Advanced Materials Research, 931–932*, 1233–1237. https://doi.org/10.4028/www.scientific.net/AMR.931-932.1233 [13]
3. Bansal, N. K., Mathur, R., & Bhandari, M. S. (1993). Solar chimney for enhanced stack ventilation. *Building and Environment*, 28(3), 373–377. https://doi.org/10.1016/0360-1323(93)90042-2 [14]
4. Černe, B., & Medved, S. (2007). Determination of transient two-dimensional heat transfer in ventilated lightweight low-sloped roof using Fourier series. *Building and Environment,* 42(6), 2279–2288. https://doi.org/10.1016/j.buildenv.2006.04.022 [23]
5. Cerdeira, F., Vázquez, M. E., Collazo, J., & Granada, E. (2011). Applicability of infrared thermography to the study of the behavior of stone panels as building envelopes. *Energy and Buildings, 43(8)*, 1845–1851. https://doi.org/10.1016/j.enbuild.2011.03.029 [3]
6. Chantawong, P. (2017). Field-measured performance of lightweight roof chimney integrated with DC fans. *Energy Procedia, 138*, 44–49. doi.org [28]
7. Chungloo, S., & Pichaisak, M. (2011). A study of the solar chimney for heat protection in a hot and humid climate. *Thammasat International Journal of Science and Technology, 6*(2). https://ph02.tci-thaijo.org/index.php/SciTechAsia/article/view/41198/34069 [12]
8. DiSalvo, F. J. (1999). Thermoelectric cooling and power generation. *Science, 285*(5428), 703–706. https://doi.org/10.1126/science.285.5428.703 [17]
9. Hasan Nia, M., Abbas Nejad, A., Goudarzi, M. M., Valizadeh, M., & Samadian, P. (2014). Cogeneration solar system using thermoelectric module and fresnel lens. *Energy Conversion and Management*, 84, 305–310. https://doi.org/10.1016/j.enconman.2014.04.041 [18]
10. Hendron, R., Farrar-Nagy, S., Anderson, R., Reeves, P., & Hancock, E. (2004). Thermal performance of unvented attics in hot-dry climates: Results from building America. *Journal of Solar Energy Engineering,* 126(2), 732–737. https://doi.org/10.1115/1.1687795 [6]

11. Khanal, R., & Lei, C. (2011). Solar chimney—A passive strategy for natural ventilation. *Energy and Buildings, 43*(8), 1811–1819. https://doi.org/10.1016/j.enbuild.2011.03.035 [15]
12. Khedari, J., Hirunlabh, J., & Bunnag, T. (1997). Experimental study of a roof solar collector towards the natural ventilation of new houses. *Energy and Buildings,* 26(2), 159–164. https://doi.org/10.1016/S0378-7788(96)01030-4 [10]
13. Khedari, J., Sangprajak, A., & Hirunlabh, J. (2002). Thailand climatic zones. *Renewable Energy,* 25(2), 267–280. https://doi.org/10.1016/S0960-1481(01)00005-2 [5]
14. Köysal, Y., Özdemir, A. E., & Atalay, T. (2018). Experimental and modeling study on solar system using linear Fresnel lens and thermoelectric module. *Journal of Solar Energy Engineering,* 140(4). doi.org [19]
15. Levinson, R., & Akbari, H. (2010). Potential benefits of cool roofs on commercial buildings: Conserving energy, saving money, and reducing emission of greenhouse gases and air pollutants. *Energy Efficiency,* 3(1), 53–109. https://doi.org/10.1007/s12053-008-9038-2 [1]
16. Maneewan, S., Hirunlabh, J., Khedari, J., Zeghmati, B., & Teekasap, S. (2005). Heat gain reduction by means of thermoelectric roof solar collector. *Solar Energy,* 78(4), 495–503. doi.org [29]
17. Michels, C., Lamberts, R., & Güths, S. (2008). Evaluation of heat flux reduction provided by the use of radiant barriers in clay tile roofs. *Energy and Buildings,* 40(4), 445–451. https://doi.org/10.1016/j.enbuild.2007.03.013 [8, 25]
18. Ogoli, D. M. (2003). Predicting indoor temperatures in closed buildings with high thermal mass. *Energy and Buildings,* 35(9), 851–862. https://doi.org/10.1016/S0378-7788(02)00246-3 [7]
19. Rangsiraksa, P. (2006). Thermal comfort in Bangkok residential buildings, Thailand. In PLEA 2006 - 23rd International Conference on Passive and Low Energy Architecture, Conference Proceedings (pp. 6–8). [4]
20. Rowe, D. M. (1999). Thermoelectrics, an environmentally-friendly source of electrical power. *Renewable Energy,* 16(1-4), 1251–1256. https://doi.org/10.1016/S0960-1481(98)00512-6 [16]
21. Santamouris, M. (2014). Cooling the cities – A review of reflective and green roof mitigation technologies to fight heat island and improve comfort in urban environments. *Solar Energy,* 103, 682–703. https://doi.org/10.1016/j.solener.2012.07.003 [9]

22. Shi, L., Zhang, G., Yang, W., Huang, D., Cheng, X., & Setunge, S. (2018). Determining the influencing factors on the performance of solar chimney in buildings. *Renewable and Sustainable Energy Reviews*, 88, 223–238. doi.org [24]

23. Sripisuttitham, S., Chantawong, P., & Bunnag, T. (2025). Experimental study of the effect of window glazing on thermoelectric power generation. *Journal Name Required*, 43, 1085–1092. (หมายเหตุ: แหล่งข้อมูลขาดชื่อวารสาร) [22]

24. Taprakone, T., & Chantawong, P. (2025a, November 18–20). *Study on the thermal performance of a lightweight solar wall chimney with a thermoelectric generation module* [Paper presentation]. The 9th RMUTR Conference and The 4th RICE & Sus–LaB 6 International Conference, Pathum Thani, Thailand. [27]

25. Taprakone, T., & Chantawong, P. (2025b, November 18–20). *The integration of fiber-cement solar chimney combined with a thermoelectric modules* [Paper presentation]. The 9th RMUTR Conference and The 4th RICE & Sus–LaB 6 International Conference, Pathum Thani, Thailand. [26]

26. Thanthong, P., Chantawong, P., & Khedari, J. (2022). Radiation-based thermoelectric power generation with finned heat absorber. *International Journal of Renewable Energy Research*, 12(1), 230–238. https://doi.org/10.20508/ijrer.v12i1.12409.g8441 [20]

27. Trans Tech Publications. (2014). 2013 *2nd International Conference on Sustainable Energy and Environmental Engineering* (ICSEEE 2013). Applied Mechanics and Materials, 521. https://www.scopus.com/inward/record.uri?eid=2-s2.0-84897625732 [21]

28. Waewsak, J., Hirunlabh, J., Khedari, J., & Shin, U. C. (2003). Performance evaluation of the BSRC multi-purpose bio-climatic roof. *Building and Environment,* 38(11), 1297–1302. https://doi.org/10.1016/S0360-1323(03)00116-1 [11]

APPENDIX A

Lists of Publication Derived from the Thesis

LISTS OF PUBLICATION DERIVED FROM THE THESIS

International Conferences	Tamnarn Taprakone, Preeda Chantawong, Study on the Thermal Performance of a Lightweight Solar Wall Chimney with a Thermoelectric Generation Module, The 9th RMUTR Conference and The 4 th RICE & Sus–LaB 6 International Conference “Green Transformation: Path a Sustainable Future” November 18 – 20, 2025.
International Conferences	Tamnarn Taprakone, Preeda Chantawong, The integration of Fiber-cement Solar Chimney combined with a Thermoelectric modules, The 9th RMUTR Conference and The 4 th RICE & Sus–LaB 6 International Conference “Green Transformation: Path a Sustainable Future” November 18 – 20, 2025.
International Journal	Tamnarn Taprakone, Preeda Chantawong, Experimental performance of a Roof Solar Concrete Chimney and Thermoelectric Power Generation, ASEAN Journal of Scientific and Technological Reports (AJSTR), (Accepted for publication,11 July 2026)

VITA

Name MR.Tamnarn Taprakone

Thesis Title DEVELOPMENT OF CONCRETE-BASED SOLAR CHIMNEY CONFIGURATIONS INTEGRATED WITH THERMOELECTRIC MODULES

Major Field Energy Engineering Technology

Biography Date of Birth : January 1, 1988

Educational Record :

2014-2015	Master of Engineering in Engineering Technology Management from King Mongkut's University of Technology North Bangkok.
2008-2009	Bachelor of Industrial Technology in Power Electronics Technology from King Mongkut's University of Technology North Bangkok

Publication :

International Conferences	Tamnarn Taprakone, Preeda Chantawong, Study on the Thermal Performance of a Lightweight Solar Wall Chimney with a Thermoelectric Generation Module, The 9th RMUTR Conference and The 4 th RICE & Sus–LaB 6 International Conference "Green Transformation: Path a Sustainable Future" November 18 – 20, 2025.
International Conferences	Tamnarn Taprakone, Preeda Chantawong, The integration of Fiber-cement Solar Chimney combined with a Thermoelectric modules, The 9th RMUTR Conference and The 4 th RICE & Sus–LaB 6 International Conference "Green Transformation: Path a Sustainable Future" November 18 – 20, 2025.
International Journal	Tamnarn Taprakone, Preeda Chantawong, Experimental performance of a Roof Solar Concrete Chimney and Thermoelectric Power Generation, ASEAN Journal of Scientific and Technological Reports (AJSTR), (Accepted for publication,11 July 2026)